8-3-2009

# Towards a universal ultra-thin fluorinated diamond-like carbon coating for nanoimprint lithography imprinters

Ryan Winfield Fillman
*Rowan University*

# TOWARDS A UNIVERSAL ULTRA-THIN FLUORINATED DIAMOND-LIKE CARBON COATING FOR NANOIMPRINT LITHOGRAPHY IMPRINTERS

by
Ryan Winfield Fillman

A Thesis

Submitted in partial fulfillment of the requirements of the
Master of Science in Engineering Degree
of
The Graduate School
at
Rowan University
August 3rd, 2009

Thesis Chair: Dr. Robert Krchnavek

ABSTRACT

Ryan Winfield Fillman
TOWARDS A UNIVERSAL ULTRA-THIN FLUORINATED DIAMOND-LIKE CARBON COATING FOR NANOIMPRINT LITHOGRAPHY IMPRINTERS
2008/09
Dr. Robert Krchnavek
Master of Science in Engineering

Nanoimprint lithography (NIL) has proven to achieve arbitrary, nanoscale features, over large areas, without the use of costly step-and-repeat UV lithography tools. The fidelity of the imprinted pattern depends on the elimination of the adhesion between the imprinted polymer and the imprinter upon withdrawal of the imprinter. The plasma deposition of a layer of fluorinated diamond-like carbon (F-DLC) has proven to be a successful anti-adhesion layer but in the past has required an entire diamond-like carbon (DLC) substrate. The requirement that the imprinter be made of DLC limits the imprinter processing and can limit the capabilities of NIL.

DLC films are considered to be an amorphous state of carbon. They have properties similar to diamond proving them to be very strong with chemical inertness and low friction coefficients due to their $sp^3$ and $sp^2$ bonds. Dopants such as fluorine can alter the chemical properties of the DLC or the surface of the DLC. The incorporation of fluorine in DLC films greatly reduces the surface free energy while retaining many of the DLC properties.

In this work, ultra-thin F-DLC is used as a NIL imprinter coating with a surface energy approaching 17.6 $mJ/m^2$ to provide a durable anti-wear, anti-stick layer. DLC is a tough coating with a low surface energy and the fluorinated self-assembled monolayer on

top of the DLC lowers the surface energy further while retaining the strength properties of the DLC. The application of an ultra-thin F-DLC anti-adhesion layer to standard NIL imprinter processing ($SiO_2$ imprinters) as well as various other imprinter material systems (inorganics, metals, polymers) has not been previously tested. It may lead to a universal and ultra-thin (<5 nm) coating for eliminating adhesion between the imprinter and the NIL sample resist.

ACKNOWLEDGEMENTS

First of all, I would like to thank my parents and sisters for all of the love and support they have given me through this challenging time in my life. Thank you all for always being there for me. I would also like to thank the entire department of Electrical and Computer Engineering faculty for their dedication and investment in my undergraduate and graduate education. In particular, I would like to thank my advisor and friend Dr. Robert Krchnavek for his support, patience, and encouragement throughout my undergraduate and graduate time at Rowan University. He introduced me to the world of nanoscience, which I am truly grateful for, and was always there to listen and give advice. I would also like to thank Dr. Shreekanth Mandayam for his guidance throughout my years at Rowan and with IEEE. He has been a great mentor and has provided me with great opportunities.

I would also like to thank the department of Physics faculty for their help in the labs and on the equipment. Particularly, I would like to thank Dr. Jeffrey Hettinger, Dr. Sam Lofland, Carl Lunk, and Ted Scabarozi. Dr. Hettinger and Dr. Lofland have given me great insight and help throughout my research at Rowan. Carl Lunk has been a lifesaver numerous times and I am thankful that he was available to help me not only run the machines but also help me fix them. Ted has given me some great insight into organization with research and has helped me with the equipment.

Finally, I would like to thank the Nanoscale Science and Engineering Initiative of the National Science Foundation under NSF Award Number CHE-0641523 and the New York State Office of Science, Technology, and Academic Research (NYSTAR) for the funding of this research.

TABLE OF CONTENTS

LIST OF FIGURES

# CHAPTER 1

## Introduction

The semiconductor industry has been the driving force behind the significant technological advances over the past 40 years. Advances in semiconductor technology and manufacturing have provided the ability to drive down the cost of transistors while shrinking the size of each individual transistor. Moore's law has become the goal of the technology manufacturing industry over the years. This law states that the number of transistors that can be placed inexpensively on an integrated circuit will increase exponentially and effectively double every 18 months. Gordon E. Moore first observed the transistor miniaturization trend in a 1965 paper in Electronics Magazine titled "Cramming more components onto integrated circuits".

To this date, the semiconductor manufacturing industry has managed to maintain this exponential curve. They have been able to produce electronics that double in performance vs. cost every two years driving technological advancements. The ability to pattern and generate electronic components of smaller size every year has been one of the main challenges to continue following Moore's law. To do this, the manufacturing industry currently uses optical lithography to transfer patterns from a mask onto a silicon wafer. Although this method has proven to be the driving force in electronic component scaling for the past 40 years, and continues to be, it has already begun to show its limitations. For this reason, new lithographic techniques have been the focus of many research groups along with the advancement of optical lithography technology.

Nanoimprint lithography has been demonstrated to be an alternative lithographic

technique for semiconductors. It has the capabilities of producing extremely small (nanoscale) feature sizes over large areas while being a less expensive alternative to the ever-increasing cost of commercial optical lithography systems (currently about $45 million) [1]. However, there are still many problems that plague this technique that must be resolved.

## 1.1 Optical Lithography

New lithography techniques are at the core of the semiconductor industry. There are many techniques available to manufacturing industries today however the most widely used technique is optical lithography. Prior to the 1970's, the majority of lithography was performed using contact or close proximity printing using blue and near UV light. This light was passed through a photomask onto a photoresist-coated semiconductor substrate. This shadow imaging process is at the core of the optical lithography concept. After the 1970's, projection printing grew substantially through the production of the Perkin-Elmer Micralign projection aligners. The primary advantage of projection lithography over contact lithography is the mask did not get dirty because it never touched the photoresist. The downside is that the optics were complex and maintaining the resolution required a small field-of-view (~ 15mm x 15mm). To remedy this, stepper systems began to be introduced in the 1980's that imaged the wafers in a step-and-repeat method. In this technique, each IC on a wafer was imaged separately with the machine controlling the location of each typically side-by-side and row-by-row. This was known as step-and-repeat due to the multiple imaging steps required to image an entire wafer along with the accurate mechanical movements needed to align one pattern on top of another for multi

layer chips. These optical steppers have been the main patterning technology for the past 30 years and will continue for as long as practical [2]. Figure 1-1 shows the basic optic components in the stepper systems.

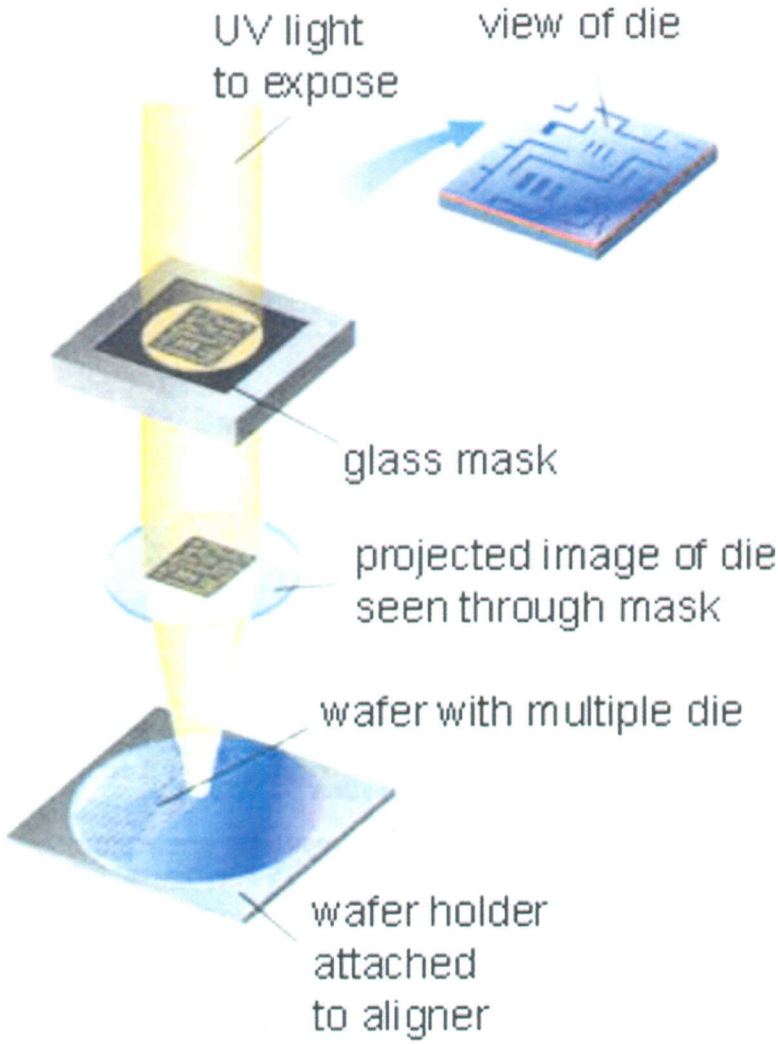


**Figure 1-1 - Optical lithography stepper basic components [2].**

Since the late 1960's, integrated circuits have been manufactured utilizing optical lithography for mass production. Since then, new techniques to improve the optical exposure tools and resists have been created with a theoretical feature size limit

approaching 10 nanometers. Despite optical lithography's limited exposure size and high tool cost, it remains the leading manufacturing tool in industry due to its high wafer throughput.

## 1.2 Imprint Lithography

Major advancements in resolution of optical lithography have historically been achieved through the use of shorter wavelengths of light. This requirement of shorter wavelengths of light has caused a significant increase in the cost of photolithographic tools. But, as shown in Figure 1-2, the increase in resolution directly translates into dramatic increases in both transistors per chip and memory density. The development of light sources and optics are responsible for the consistent increase in manufacturing cost. For instance, 193nm immersion has increased the costs of the lens and extreme ultra violet lithography (EUVL) is expected to continue the increase in cost [1]. Industry is currently working with 193nm immersion to achieve 45 and 32nm feature sizes. A transition to 10-14nm EUVL is planned since 157nm $CaF_2$ has been removed from Intel's Next Generation Lithography (NGL) roadmap [3].

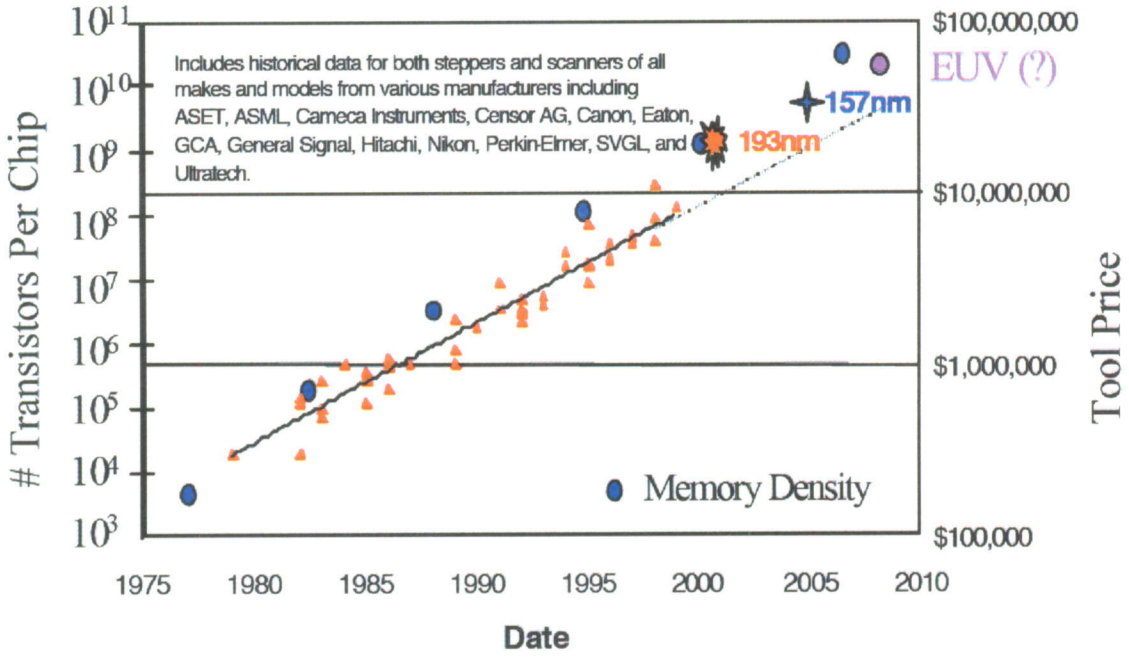


**Figure 1-2 - Transistor density and tool price as a function of date [3].**

Imprint lithography uses a physical imprinting process instead of optical pattern transfer. In this process, a 3-dimensional mask pattern is etched into the surface of the imprinter material. This pattern is then transferred by physically pressing the mask against the surface of the wafer that has been coated with a material that allows for the pattern to be transferred. The wafer can be coated with a chemical layer that catalyzes a chemical reaction in the resist allowing for the pattern to be developed [1]. An alternative method, as used in this work, uses a thin organic layer. In this method, the imprinter is pressed into the wafer allowing for the organic layer to conform to the three dimensional pattern from the imprinter. The substrate can be heated to a liquid state and then cooled to harden the pattern. A room temperature, light sensitive, liquid can also be exposed to a bright ultraviolet light source through a transparent mask hardening the organic material. When

heat is used, the organic layer can be cooled to allow the organic layer to harden in the inverse pattern of the imprinter. Imprint lithography removes the limitations on feature size of optical lithography as well as limitations on patterning large areas or wafers. It allows for feature sizes less than 10nm over entire wafers but not without implications [4]. When the liquid is hardened and the mask is pulled away, the pattern has a tendency to stick to both the silicon and the imprinter. This causes the pattern to rip causing poor pattern transfer and possibly destroying the imprinter. Other problems with this technique include alignment, hardening, surface wetting, and mask separation. The requirements of the imprinting process will cause this technique to take more time for alignment than the quick optical methods. However, NIL does allow for much smaller feature sizes over larger sample sizes than optical lithography at a significantly reduced expense. Figure 1-3 is a brief overview of different NIL techniques.

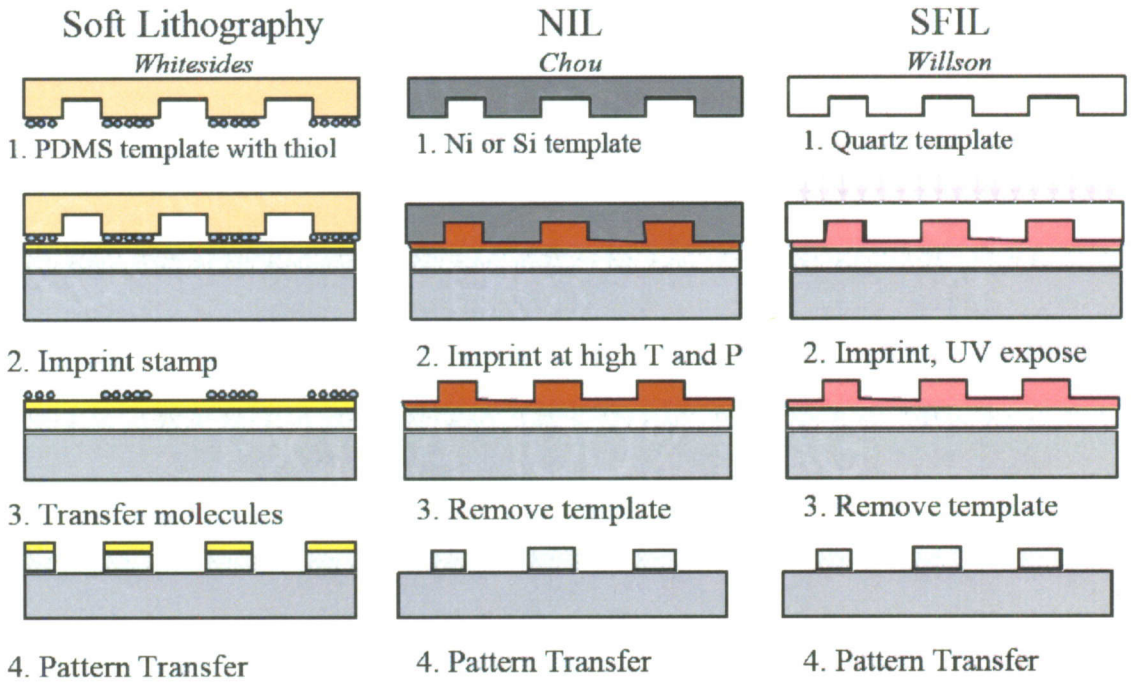


**Figure 1-3 - Variations on the NIL technique [1].**

In this work, a slight modification of Chou's process is used. A silicon dioxide on silicon imprinter is used with 2% PMMA in Chlorobenzene as the organic material on the substrate. An anti-adhesion layer is also described that eliminates the adhesion of the imprinted polymer to the imprinter.

## 1.3 Current Applications of Imprint Lithography

Imprint lithography has many possible applications in the semiconductor and electronics manufacturing areas. There are a number of companies that are currently selling imprint tools such as Nanonex, Obducat, EV Group, Suss Microelectronics, NND, Hitachi and Jenoptiks [4]. Obducat has developed thermal imprint tools capable of patterning wafers up to six inches in diameter. It operates at temperatures and pressures as high as 350°C and 80 bar as well as having the ability to imprint both sides of a wafer. EV Group is offering the EVG520HE that is a thermal imprint tool capable of operating at temperatures as high as 550°C and 40 bar. Suss offers similar tools, the SB6E and MA6, and has recently released the Stepper 200 that can operate as either a thermal or UV imprint tool with imprint times less than 1 minute per wafer [4]. In the United States, the company Nanonex offers thermal imprint tools. The NX-3000 from Nanonex allows for alignment and can handle substrates as large as 200mm. One advantage of the Nanonex tools is that they apply an air-cushion press (ACP) to uniformly apply pressure when contacting the template and wafer [4]. Two companies from Asia also offer commercial imprint systems such as NND out of Korea and Hitachi from Japan. NND has the Nanosis 610 that is designed for wafers up to 150mm in diameter and Hitachi has a new thermal imprint system that can handle full wafers up to 300mm in diameter. Hitachi is

currently utilizing these technologies for fabricating patterned magnetic media such as magnetic hard drives and continue to modify and improve their designs.

## 1.4 Summary

As optical lithography processing techniques evolve and continue to increase in initial cost, alternative next generation lithography (NGL) tools will be needed to keep the cost of advanced electronics appealing. The limited pattern size for optical lithography may also drive companies to begin investing in other NGL tools. Nanoimprint lithography tools appear to have the highest potential to replace optical lithography, however there are still many problems that need to be overcome. These issues deal mainly with the direct contact between the imprinter and the substrate along with the required alignment. These will need significant research to eliminate these issues for wide commercial application in manufacturing. While NIL has been emphasized as a technique to replace optical lithography, the ability for NIL to pattern entire wafers in a single step opens up new opportunities for technological advancement. For example, Hitachi is currently using the NIL technique for patterning magnetic hard drives allowing for a significant increase in bit density. NIL is very practical for the hard drive manufacturing industry since it does not require the alignment of multiple layers such as in the semiconductor manufacturing industry. Furthermore, this could not have easily been achieved using optical lithography because of stitching (misalignment) errors between patterns in the step-and-repeat process. Imprint lithography has the potential to impact several technological areas, such as mechanical or biological, because of the nanoscale resolution over very large areas.

# CHAPTER 2

## Nanoimprint Lithography Background and Implementation

### 2.1 Chapter Overview

Nanoimprint lithography has been briefly discussed in the introduction of this thesis. This chapter provides a more detailed description of nanoimprint lithography along with the techniques that have been and are utilized at Rowan University. Advantages and disadvantages are also given for current anti-stick coatings used in NIL processing and for those previously investigated at Rowan University.

### 2.2 Introduction

As stated before, imprint lithography utilizes a physical imprint process instead of optical pattern transfer. A 3-dimensional mask pattern is etched into the surface of the $SiO_2$ on Si imprinter material and transferred by physically pressing the mask against the substrate. The substrate surface contains a thin layer (~100nm) of 2% polymethymethacrylate (PMMA) in chlorobenzene that is heated above the glass transition temperature while applying pressure between the imprinter and the substrate. This allows the PMMA to flow and conform to the three dimensional pattern on the imprinter. After a sufficient amount of time, the imprinter and substrate are then cooled to room temperature and the imprinter is removed leaving the transferred pattern behind in the PMMA on the substrate. Figure 2-1 shows a graphical representation of each step of the imprinting process.

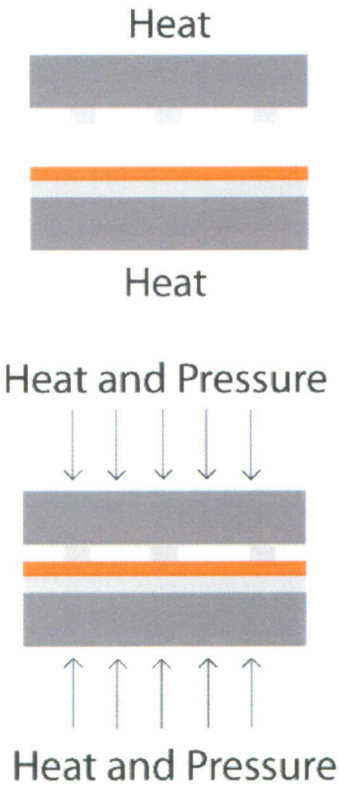


Both the imprinter and the sample are first heated above the PMMA transition temperature, 105°C, to 170°C

Pressure is then applied between the imprinter and the sample while maintaining the heat at 170°C for 5 minutes. The first minute is a pressure ramp starting at 10 psi and ending at 40 psi. The pressure is then held at 40 psi for 4 minutes.

After the 5 minute pressure stage, both the imprinter and sample are allowed to cool to 30°C

Once the imprinter and sample reach 30°C, a small ramping pressure starting at 10 psi is applied to separate the two substrates. This pressure is increased as needed to aid the separation.

**Figure 2-1 - Basic NIL processing with thermal imprinting.**

This method allows for feature sizes less than 10nm, but the feature size is dependent on the method of patterning the imprinter. There are many advantages and disadvantages to this method of lithography and they will be addressed later in this chapter. An anti-adhesion layer can solve some of the problems with NIL but many anti-stick coatings are unreliable or can cause pattern defects.

## 2.3 Imprinting Machine Designs

The imprinter applies controlled pressure and controlled heat to both the imprinter and the sample (polymer coated substrate). Dan Marks designed the original imprinter in 2005 at Rowan University [5]. This design was a large and heavy structure with two parallel plates where the top plate could be controlled with pressurized nitrogen. The original imprinter design can be seen Figure 2-2.

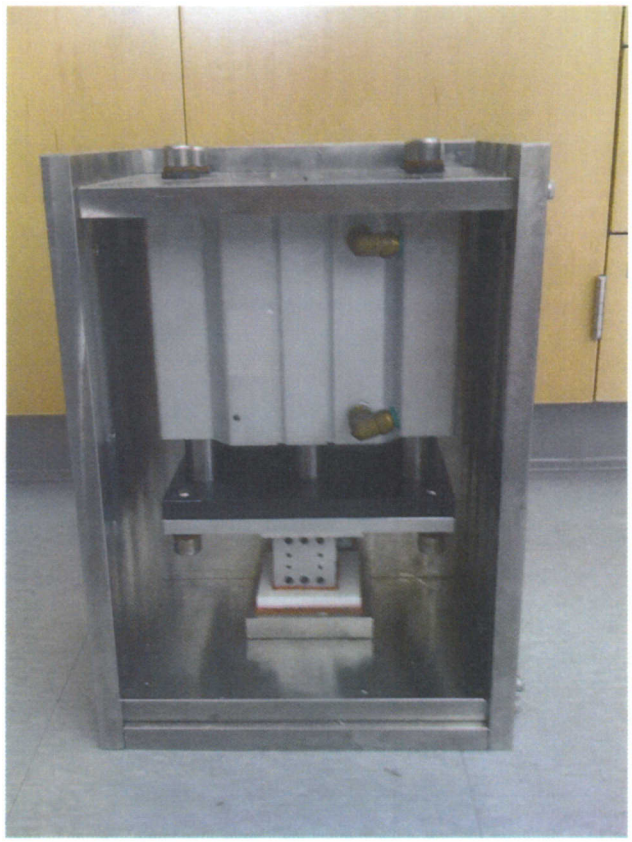

**Figure 2-2 - Original imprinter design created by Dan Marks.**

The imprinter has a stainless steel frame with a Parker P5T Series pneumatic press that utilized nitrogen to apply pressure between the imprinter and the substrate. The bottom of the pneumatic press and the top of the bottom steel plate have a white block of Macor® and an aluminum block attached to them [6]. The Macor® block is utilized due to its low thermal conductivity, 1.45 W/m-˚C, to isolate the high temperatures required for the imprinting blocks from the rest of the stainless steel structure. High temperature, room temperature vulcanizing (RTV), adhesive is used to attach the Macor® to the frame and the aluminum block to the Macor®. The aluminum blocks have 3 large holes for the heating elements and 2 small holes for the thermocouple feedback to control the temperature across both the top and bottom aluminum blocks. The temperature of these

blocks is controlled through WATLOW SERIES 93 temperature controllers and an additional switch on the control box designates the direction of the pneumatic press. The original controller design also utilized controls for timed heating and cooling, but these were removed due to problems with the system. After this original imprinter was designed, two other versions of the imprinter were created. One of these models was the same design but on a smaller scale for smaller wafer imprinting. The third imprinter design, developed by Brian Balut and Ray Odgers, included an active cooling system and was slightly larger than the small imprinting press design. This imprinter is the model that was used through this research due to the ability to include active cooling and can be seen in Figure 2-3.

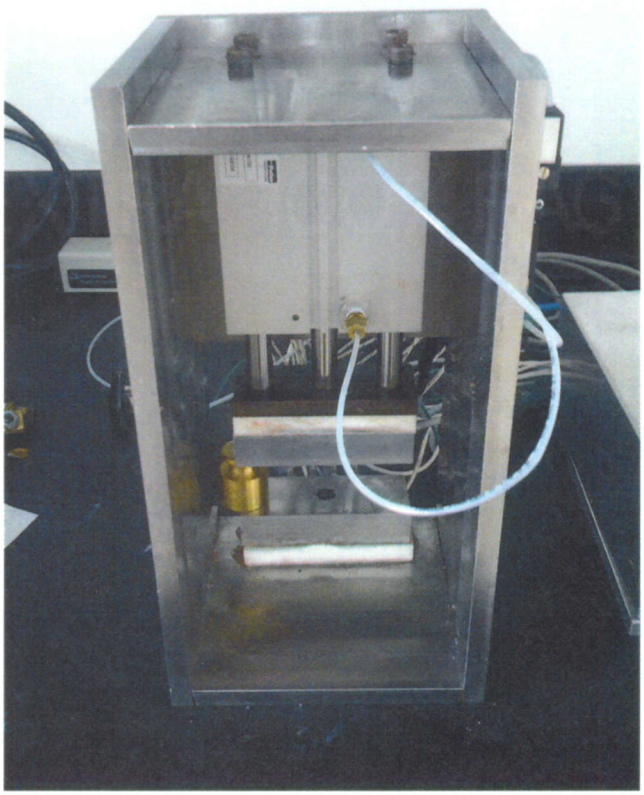

**Figure 2-3 - Current imprinter design.**

The active cooling modification included two copper pipes that were connected to either side of the lower aluminum block and the block was hollowed out to allow air or water flow through the block. Although the ability to water cool the substrate would have sped up imprinting times, the copper pipes were removed since it was not an essential part of the imprinter. The modified control box can also be seen in Figure 2-4 where only the essential parts to the imprinting process were kept.

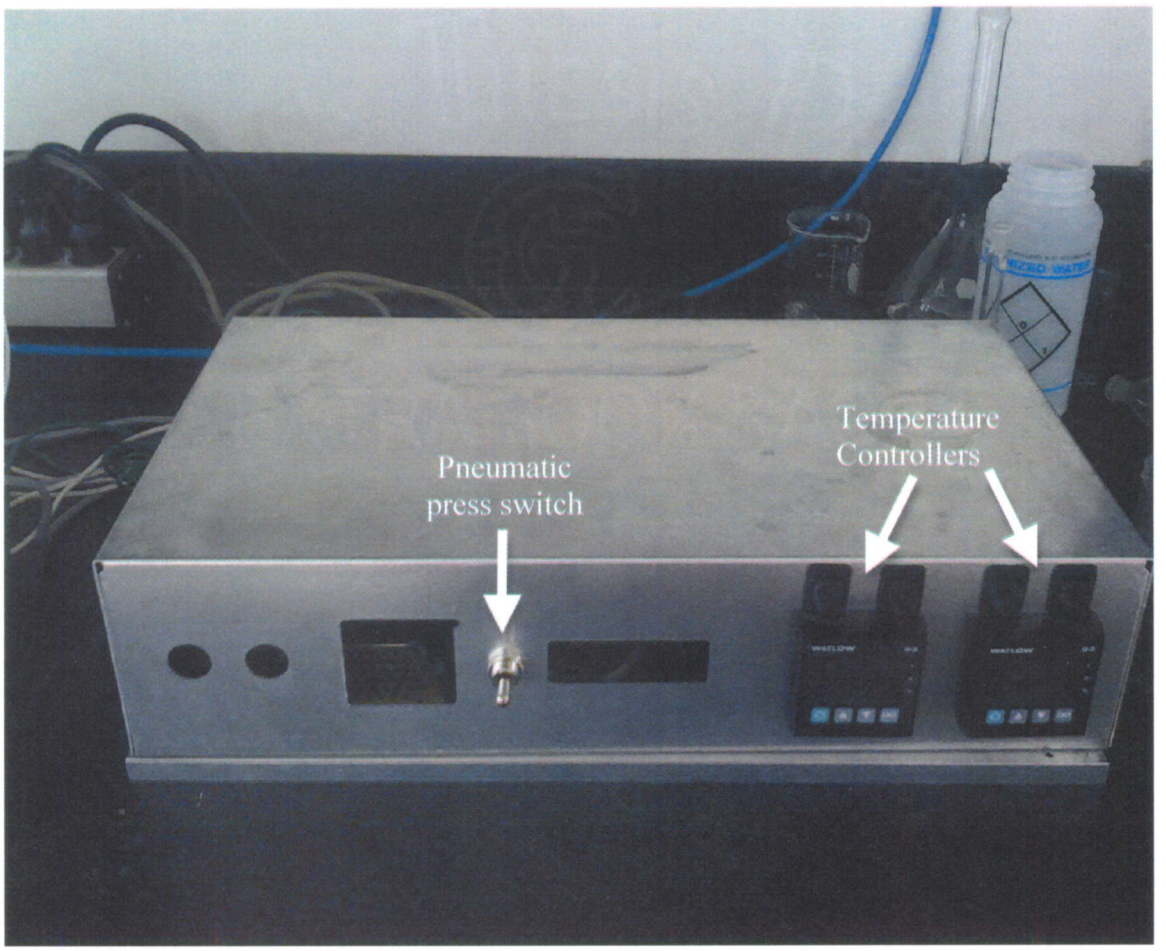


**Figure 2-4 - Current imprinter control mechanism.**

The metallic switch near the middle of the control console dictated the direction of the pneumatic press. The direction of the press was controlled through the use of a single solenoid spool valve. This valve, when enabled or disabled, controls the direction of the piston. The two control boxes on the right control the temperatures of the top and bottom aluminum blocks allowing for individual temperature control of each block.

## 2.4 Imprinter

Electron-beam lithography was utilized to generate the initial pattern on the imprinter for NIL. This technique was used due to its capabilities of high-resolution pattern generation and ability to customize the types of patterns on the $SiO_2$/Si (250nm thermally grown $SiO_2$ on silicon) imprinters. First, 10mm x 10mm $SiO_2$/Si substrates were cut and cleaned thoroughly using sonication, acetone, and methanol. Previous research had used mechanical cleaning of the substrates, but the lint free cloths would typically leave particles on the substrate that would cause streaking when applying the PMMA layer. For this method, the $SiO_2$/Si substrates were placed in a beaker of acetone and sonicated for 5 minutes in an AQUASONIC model 50T as seen in Figure 2-5.


**Figure 2-5 - Aquasonic model 50T sonication unit.**

Post sonication, the samples were taken out of the acetone bath and sprayed with methanol before being dried with dry nitrogen gas. This process proved superior to the mechanical cleaning method. It also provided PMMA layers on the $SiO_2$ that are very smooth and no detrimental defects.

After cleansing, the samples were coated with 2% polymethylmethacrylate (PMMA) in chlorobenzene, a typical electron beam resist. Two layers of PMMA were used to increase the resolution of the pattern exposure and to aid in the subsequent liftoff

The first layer of PMMA was 100k PMMA and the second layer was 950k PMMA, where 100k and 950k represent the molecular weight of the PMMA. The 100k PMMA was spun onto the substrate for 45 seconds at 4000rpm, using a Laurell spinner, to generate a 50nm layer of PMMA. It was then heated on a Barnstead Thermolyne hot plate to 180°C for 2 minutes. After the substrate cooled, the second layer of 950k PMMA was spun onto the substrate for 45 seconds at 4000rpm for a thickness of approximately 50nm. The substrate was then heated again to 180°C. Both of the resists were spun onto the $SiO_2$/Si substrate at 4000rpm for 45s to generate a total layer thickness of approximately 100nm.

The sample was e-beam written using a Nanometer Pattern Generation System (NPGS) from JC Nabity Lithography Systems in Bozeman, Montana on a LEO 1530VP SEM. The NPGS software has the ability to control the electron beam of the SEM to manipulate the location of the electron beam while exposing the e-beam resist (PMMA) in those locations. One problem that arises when controlling the e-beam of the SEM is the degree that the focus changes from one point to another on a substrate. This is due to the optics of the electron beam and the degree that the substrate is not perfectly perpendicular to the e-beam. The NPGS software allows for the calibration of the focus of the e-beam across the substrate by performing calculations based on 4 or 5 focal points around the substrate. Since the PMMA surface of the substrate is very smooth, 50nm gold colloids are placed at each of the 4 corners of the substrate before placing it in the SEM. This provides 4 focal points at the extremities of the substrate for generating the focal plane with the NPGS software. Each point was focused at 300,000x to allow for more accuracy in the NPGS software calculations. After the NPGS software calculates the plane, it is

important for the RMS error term to be less than 0.001 to ensure a focused beam across the substrate.

All patterns were generated using 30kV on a 30μm aperature with a working distance of approximately 6mm. The working distance of 6mm is used as a compromise between tighter focal point at shorter working distances and larger depth of field at longer working distances. The patterns generated using the NPGS system were 100μm x 100μm squares with arrays of dots less than 30nm in diameter and a pitch of 100nm. Figure 2-6 shows the array of 30nm dots that were generated within the 100μm x 100μm squares.

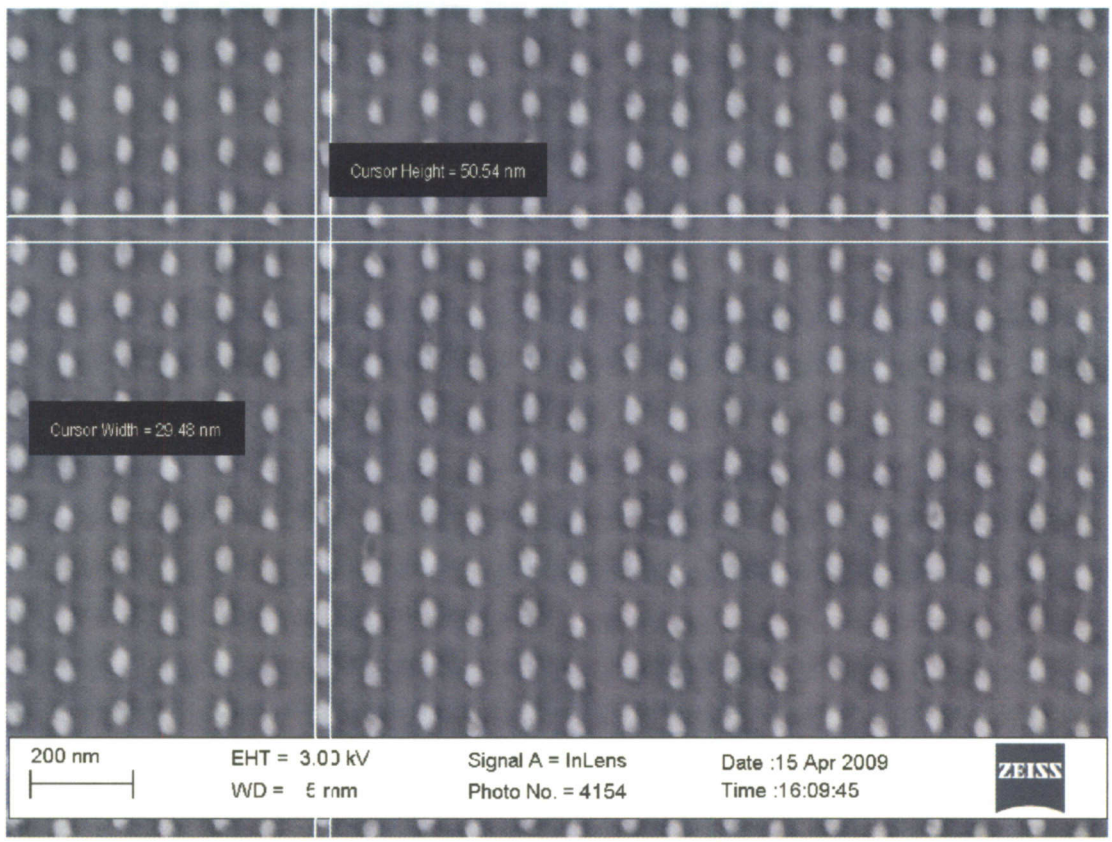


**Figure 2-6- Pattern generated using EBL with approximately 30nm diameter dots separated by approximately 50nm from each other.**

After the patterns were exposed by the e-beam of the SEM, they were developed in a 1:3 mixture of MIBK:IPA for 60 seconds. Since PMMA is a positive e-beam resist, the pattern that was exposed by the e-beam of the SEM became soluble in the developer and was removed from the $SiO_2$/Si substrate. The MIBK:IPA solution did not remove the unexposed PMMA leaving the desired pattern generated by the NPGS system surrounded by PMMA.

Following the exposure and developing of the substrate, it was then placed in a thermal evaporator for the deposition of approximately 20nm of chrome. The chrome was evaporated onto the substrates using an Edwards E306A coating system by passing large current through a chrome coated tungsten rod. The deposition rate was approximately 0.2 nm/min. This evaporation process coats both the PMMA and exposed $SiO_2$ with a layer of Cr without coating the sidewalls of the PMMA. The thickness of the Cr layer is critical when compared to the thickness of the PMMA. For the liftoff of the PMMA, it is very important to ensure that the Cr on top of the PMMA is not connected to the Cr on top of the $SiO_2$. For this reason, the thickness of the Cr layer must be less than 1/3 the total thickness of the PMMA layer. Liftoff was performed in a 1:1 mixture of methylene chloride and acetone. This removed the PMMA while removing the Cr that was on top of the PMMA. Sonication was used along with the liftoff process to help remove the PMMA with the Cr on top. Sonication times were typically kept under 1 minute to help protect the small (<30 nm) Cr features from ripping from the $SiO_2$ substrate surface. As the feature sizes decrease, the sonication has a higher probability of destroying the Cr features due to the fixed amount of energy that is transferred to these smaller features. Figure 2-7 shows the pattern generated after Cr deposition and liftoff of the unexposed

PMMA and Cr. This leaves the pattern, exposed by the NPGS SEM system, in chrome and the surrounding areas removed to expose the $SiO_2$ surface.

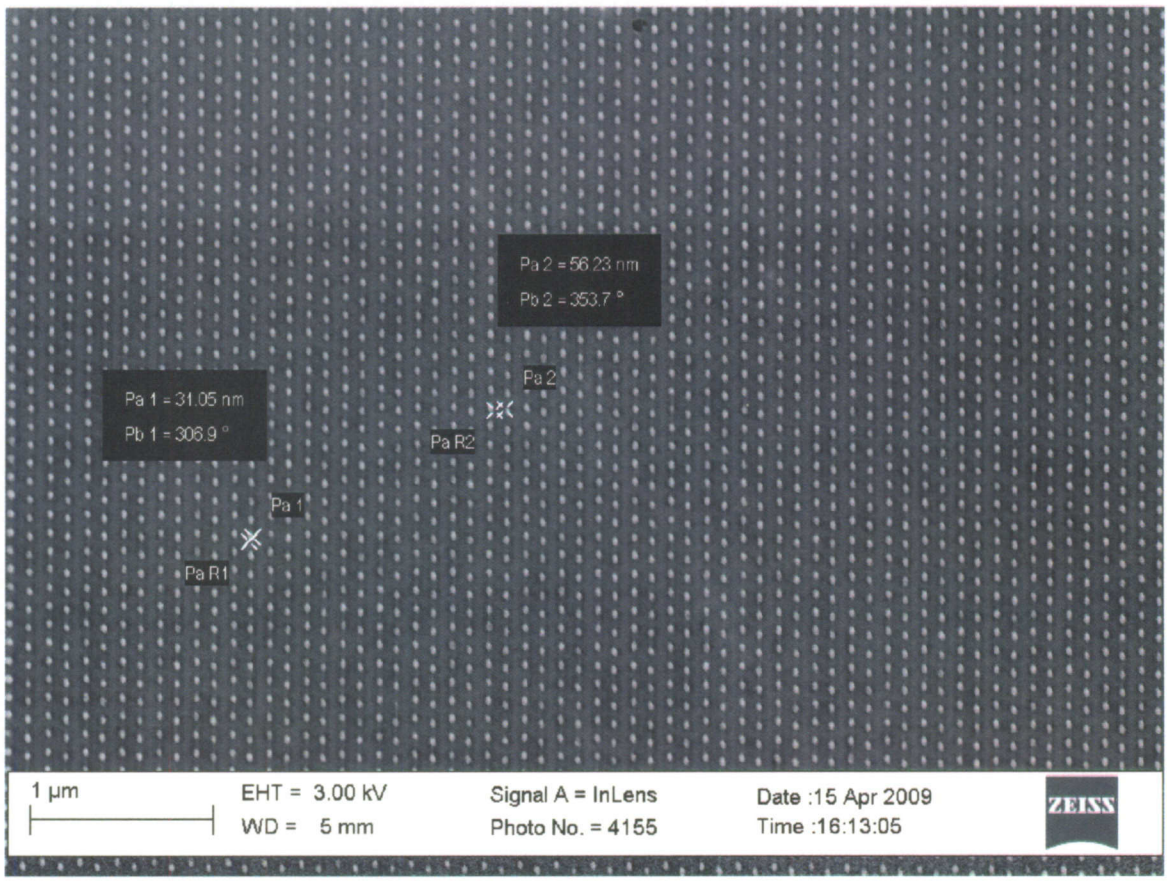


**Figure 2-7 - Patterns generated were sets of 100µm x 100µm squares with the dot pattern shown above in this 5µm x 5µm SEM image.**

Following the generation of the nanometer-sized Cr dots, the sample was subjected to reactive ion etching in an Oxford Plasma Lab 80+ Reactive Ion Etcher (RIE) as seen in Figure 2-8.


**Figure 2-8 - PlasmaLab 80+ Reactive Ion Etcher.**

The plasma was formed using a combination of $CF_4$ and $H_2$ gas with a flow rate of 40SCCM and 12SCCM respectively. The process uses a forward bias voltage generating a power of 40W for 5 minutes resulting in pillars with a height of 150nm. This combination anisotropically etched the oxide layer leaving the Cr intact. With an etching

time of 4 minutes, the pillars created were about 100nm in height with a diameter the same of the Cr dots (30nm). Each imprinter contained a pattern of 100 of these 100μm x 100μm squares (10 x 10 pattern of squares) with 30nm diameter pillars of 100nm height filling each square. This provided a vast number of pillars ($10^8$) to inspect on each sample for the imprinter analysis post imprinting as seen in the results.

## 2.5 Imprinting

The preparation of samples to be imprinted was similar to the preparation for the e-beam writing. Two layers of PMMA were spun onto the sample at 4000 rpm to produce a total thickness of about 100nm. These two layers of PMMA help with the liftoff process of the PMMA for the use of the substrates as patterned magnetic material or other processing. The imprinting was performed in a custom built imprinting press as described earlier in this chapter. The imprinter was placed in the top press with the lower press containing the sample to be imprinted. Both sample and the imprinter were then heated above the glass transition temperature, nominally 105°C, to 210°C through the use of heaters in each of the aluminum plates. It is important to pass the transition temperature of the PMMA to allow fluid motion of the PMMA while not heating the substrates far above 230°C due to the potential degradation of the PMMA. Double sided adhesive conductive carbon discs were utilized for attaching the imprinter and sample to the aluminum plates. The carbon discs provide an excellent method for attaching the imprinter and sample to the aluminum plates while enabling a degree of flexibility and cushion between the $Si/SiO_2$ wafers and the aluminum plates. Previous research for the imprinter press by Dan Marks had proved that 170°C at 40psi for 4 minutes was an optimal imprinting

temperature, pressure, and time for the imprinter and sample using the smaller imprinter press design [5]. Due to the use of the alternate imprinter design, these optimal imprinting factors had to be recalibrated and it was found that 210°C was a better temperature for a similar imprinting pressure and time. After both the sample and the imprinter were above the glass transition temperature, the press was released allowing the samples to come into contact with each other with an initial pressure of 10 psi. The pressure was gradually increased to 40 psi over a time period of 1 minute forcing the imprinter into the sample while maintaining the temperature of both the imprinter and the sample. After 4 additional minutes, both the imprinter and sample were cooled to about 30°C before separating the sample from the imprinter. This process is similar to that developed by Dan Marks during his work at Rowan University with only a temperature modification required due to the modification of the imprinter design [5]. Instead of increasing the temperature of the imprinter and the sample, it is also possible to increase the pressure or imprinting time to produce similar results. However, increasing the pressure between the imprinter and the sample resulted in a higher probability of the $Si/SiO_2$ imprinter or sample breaking under the additional pressure. Increasing the imprinting time was a viable method to allow for the imprinter features to penetrate the PMMA, but increasing imprinting time is not desirable. The higher temperature used in this work allowed for a similar imprinting time and lower pressure during the imprinting process while not degrading the PMMA on the sample to be imprinted.

## 2.6 Nanoimprint Lithography Drawbacks

Although nanoimprint lithography will allow for much smaller features than optical lithography, there are still many drawbacks to the technique that will need to be addressed. To investigate the PMMA flow, two techniques have been tested with the imprinted substrate. When the PMMA is baked after spinning but prior to imprinting, pressures on the scale of 90psi are needed to transfer the pattern along with higher temperatures on the order of 210°C. However, this technique does lower the chances of the PMMA sticking to the imprinter. On the other hand, if the PMMA is not baked prior to imprinting, there is a higher probability of the PMMA sticking to the imprinter. However, lower temperatures and pressures around 170°C and 40psi are required to transfer the pattern when pressure is applied between the imprinter and the sample during heating. It is believed that this is due to the chlorobenzene that is still in the PMMA allowing it to flow better at lower temperatures making it easier to transfer the pattern.

However, this also is problematic since the PMMA can sometimes flow too much causing limited pattern transfer. Previous research has shown that resist flow can be enhanced if the solvent is still present in the resist. In this research, room temperatures were used to transfer the pattern into the solvent enhanced resist (Shipley, S1813) [7]. The problem of the PMMA sticking to the imprinter post cooling of the substrate is a major issue in nanoimprint lithography that needs to be addressed and the increased flow of the solvent enhanced resist increases the probability of adhesion to the imprinter. Alignment issues are another problem with nanoimprint lithography. It has been found that poor alignment of the imprinter to the substrate sometimes causes the substrate or the imprinter to break during the imprint process. One solution to this problem that has been

found is to always use a substrate that is larger than the imprinter. This also helps with the buildup of PMMA on the edges of the substrate (edge bead) that can also cause the substrate to break due to the different heights of the PMMA. It is also known that nanoimprint lithography takes a couple minutes to process due to the time needed to heat and cool the substrate. One solution to this is to add the cooling system back to the imprinter, but this still requires minutes to transfer the pattern as opposed to optical lithography that takes mere seconds. Some researchers have switched to a process called Step and Flash Imprint Lithography (SFIL). SFIL does not require the heating and cooling of the substrate but it does use a UV curable etch barrier that is not easily removable with a solvent. Essentially, SFIL is the same as NIL except that the UV resist is photo sensitive, liquid at room temperature and only hardens when exposed to a UV light source. This causes the imprinter design to be more expensive since it utilizes a UV light source although it is still much cheaper than the current light sources used in optical lithography. SFIL does have the added advantage that the imprint process takes less time and alleviates the problems due to thermal distortion of the resist on the substrate.

## 2.7 Current Mold Anti-Stick Coatings

It is well understood that Mold Release Coatings (MRC) are necessary in NIL. The MRC helps prevent the adhesion of the substrate polymer to the imprinter when the imprinter comes into contact with the substrate polymer. As the feature sizes get smaller on NIL, the MRC becomes more important because the smaller features increase the surface area of the imprinter. All release coatings provide a method for lowering the surface energy of the imprinter through molecules that covalently bond to the surface of the imprinter. Van

der Waals Forces are the main forces that must be overcome on the surface of the imprinter since it is intermolecular in nature. Molecules with weak dipoles are very important for anti-stick properties of imprinters. The C-F bond is a very strong and stable bond and therefore, fluorine coatings are the main research area for use in anti-stick coatings. A similar type of coating in use in the kitchen is PTFE, or better known as Teflon®. While Teflon® acts as a great anti-stick layer on kitchen pots and pans, it has a surface tension of 18 $mJ/m^2$. One release agent that has been utilized in SFIL is tridecafluoro-1,1,2,2-tetrahydrooctyltrichlorosilane (trichlorosilane or TCS) and was proven to have a surface tension closer to 12 $mJ/m^2$ [8]. Previous work at Rowan University by Robert Grove utilized TCS that was purchased from the American division of Gelest. One disadvantage of this coating is that it cannot be applied simply to the $SiO_2$ surface of the Si imprinters. Therefore, the surface had to be treated with nitric acid for 5 minutes to hydroxylate the surface of the $SiO_2$ meaning that the Si-O-Si bonds had to be replaced with 2 Si-OH bonds. Although this technique has been proven to work well most of the time, there were times when the substrate polymer still stuck to the imprinter. Also, this process of treating the imprinter with TCS is a lengthy process that involves acids, removal of water, and heating the imprinter to over 250°C and working in a glove box. This has the potential to damage the imprinter especially when small feature sizes are present on the imprinter. Failure to keep the TCS dry could also damage the anti-stick layer requiring a new imprinter to be fabricated. Although this anti-adhesion technique works well most of the time, there is much room for improvement and creating a simpler process for applying a MRC is needed.

Fluorination of surfaces can also be achieved by the use of $CF_4$ plasma or other

fluorocarbon based plasma. Previously $CF_4$ has been used for etching and fluorine contamination has always been seen as an adverse effect. However, this technique has also been used for imprinters to create a hydrophobic surface lowering the surface energy of the imprinter. This technique has been applied to $SiO_2$ as a simple fluorine treatment and also as a Fluorinated Diamond-Like Carbon (F-DLC) coating. The problems with these techniques are that the fluorine treatment of $SiO_2$ weakens the imprinter features as well as weakening the diamond-like properties of DLC when the fluorine is incorporated into the DLC layer [9]. $CF_4$ plasma treatment has also been used for DLC substrates to lower the surface energy. This protects the desired properties of DLC while lowering the surface energy but the treatment has always been performed on DLC substrates and not on $SiO_2$/Si substrates. This limits the imprinter material to DLC substrates as seen in previous research [10].

## 2.8 Previous Work

Previous graduate students, Dan Marks [5] and Robert Grove [11], have performed a large amount of research in the field of NIL at Rowan University. The primary goal of Dan Marks thesis was to sputter Permalloy, a magnetic material, on top of the polymer with closely packed holes. Much of his research dealt with the magnetic testing of these Permalloy dots to see if they could be used for magnetic storage. The Permalloy was determined to be too soft for magnetic force microscopy (MFM) but he was able to design the first two imprinters at Rowan University [5]. During Robert Grove's research time at Rowan University, Brain Balut and Ray Odgers designed the first active cooling nanoimprint lithography system that was proven to reduce the cycle time of NIL. Robert

Grove's goal for his thesis was to utilize Hydrogen Silsesquioxane (HSQ) to fabricate the imprinter. HSQ acts as a negative e-beam resist and simplifies imprinter fabrication considerably. Robert Grove's research with HSQ evaluated the time-dependent and instability properties of the HSQ while developing a method to pattern magnetic media [11].

## 2.9 Summary

Nanoimprint lithography has the potential to increase the density of magnetic hard drives as well as provide a new lithographic technique for generating patterns with smaller features than optical lithography. There are still many problems with NIL, but many have been addressed at least to provide a better solution. However, one of the problems that still plagues NIL is a simple and reliable method to remove the adhesion of the polymer on the substrate to the imprinter. It has been proven that a fluorine surface can lower the surface energy of an imprinter but the methods for application are time consuming and are not consistent while potentially damaging the imprinter during the processing. This thesis provides a possible solution to this problem through the use of a novel ultra-thin DLC and F-DLC coating of the $SiO_2$/Si imprinter along with an approach towards creating a universal anti-adhesion technique for other imprinter materials.

# CHAPTER 3

## Diamond-Like Carbon on Silicon Dioxide

### 3.1 Chapter Overview

This chapter reviews many of the desirable properties of Diamond-Like Carbon (DLC). Many of the problems with analyzing ultra-thin layers of DLC are also addressed and some research has made it possible to understand the excellent mechanical properties of even ultra-thin DLC. A technique is also described for the deposition of a uniform ultra-thin (< 5nm) layer of DLC as well as tests for the adhesion of this film to $SiO_2$ surfaces since this has not been tested in previous research. The properties of this ultra-thin layer are also analyzed and tested mainly for surface energy properties.

### 3.2 Introduction

Diamond-Like Carbon (DLC) has many applications including anti-static, anti-wear, anti-fouling, anti-corrosion, and as gas permeation barriers [12]. DLC is an amorphous form of carbon that closely resembles diamond in its hardness, lubricity, and resistance to chemical attack. Most of these applications require films that are < 100 nm in thickness that are difficult to analyze. These problems stem from difficulties in measuring the film thickness and the fact that the film properties have to be measured with adequate surface sensitivity.

## 3.3 History of Diamond-Like Carbon

Carbon can exist in several allotropes including graphite, diamond, fullerenes, and carbon nanotubes [12]. If the processing conditions are chosen properly for the deposition of carbon films, it is possible to obtain a purely amorphous carbon phase. DLC is a term used to describe all amorphous carbon that has a high degree of $sp^2$ (trihedral) and $sp^3$ (tetrahedral) bonding [12]. Research on DLC films has been performed for almost 40 years. In 1971, the first report of DLC films was by Aisenberg and Chabot [13]. Interest in these amorphous carbon films stems from their unusual properties including being resistant to chemical attack, high hardness, and good optical transparency. Along with these properties, it can also be deposited at low temperatures making it compatible with a wide range of materials. Some materials that have been found to be incompatible with the plasma growth of DLC include common metals such as copper, gold, and nickel [14]. The bonding of DLC to Si surfaces has proven to be excellent but there has not been research on the bonding quality between DLC and $SiO_2$. This is addressed later in this chapter utilizing a qualitative method for determining the adhesion.

## 3.4 Previous Work

Raman microscopy, electron energy loss spectroscopy (EELS), X-ray reflectometry (XRR), spectroscopic ellipsometry (SE), X-ray photon electron spectroscopy (XPS) and surface Brillouin scattering (SBS) have all been used to test films as thin as 10nm although the data is not always quantitative [12]. Previous work [12] has been performed to study the intrinsic mechanical properties of ultra-thin DLC films using nanoindentation data, Raman spectroscopy, optical interferometry, and X-ray reflectometry. In this work,

it was concluded that the properties of amorphous carbon films on Si get denser, stiffer, and harder as they get thicker. These calculations were performed on film thicknesses varying from 2.2 nm up to 100 nm. However, it was also noted that the deposition technique also determines if this is the case leaving opportunity for other deposition techniques to not have this common property with ultra-thin films of DLC. One deposition technique where this property of increasing hardness of the DLC film was not found was with the sputter deposition techniques [12]. An important property of DLC is that the hydrogen content is very important to the hardness of the DLC films. Less hydrogen content resulted in the formation of carbon double bonds but also increases the graphitic content of the DLC layer [12]. In this research, the ultra-thin DLC films were sputter deposited with low hydrogen content, so it is believed that it still retains some of the hardness properties of the bulk DLC films. However, this was not directly tested with our deposition technique and it would involve an extensive research project in itself.

## 3.5 Ultra-Thin Deposition Technique

In this research, the ultra-thin DLC was deposited using a TM Vacuum Rotating substrate Sputter Deposition System with a carbon target. A forward power of 200 Watts and bias power of 30 Watts was used at room temperature under a pressure of 6mTorr with an Ar:$H_2$ flow rate of 30sccm and 9sccm respectively. This system configuration generated a 4nm/minute deposition rate on the rotating sample tray. Figure 3-1 shows the DLC thickness as a function of the deposition time showing an approximately constant deposition rate.

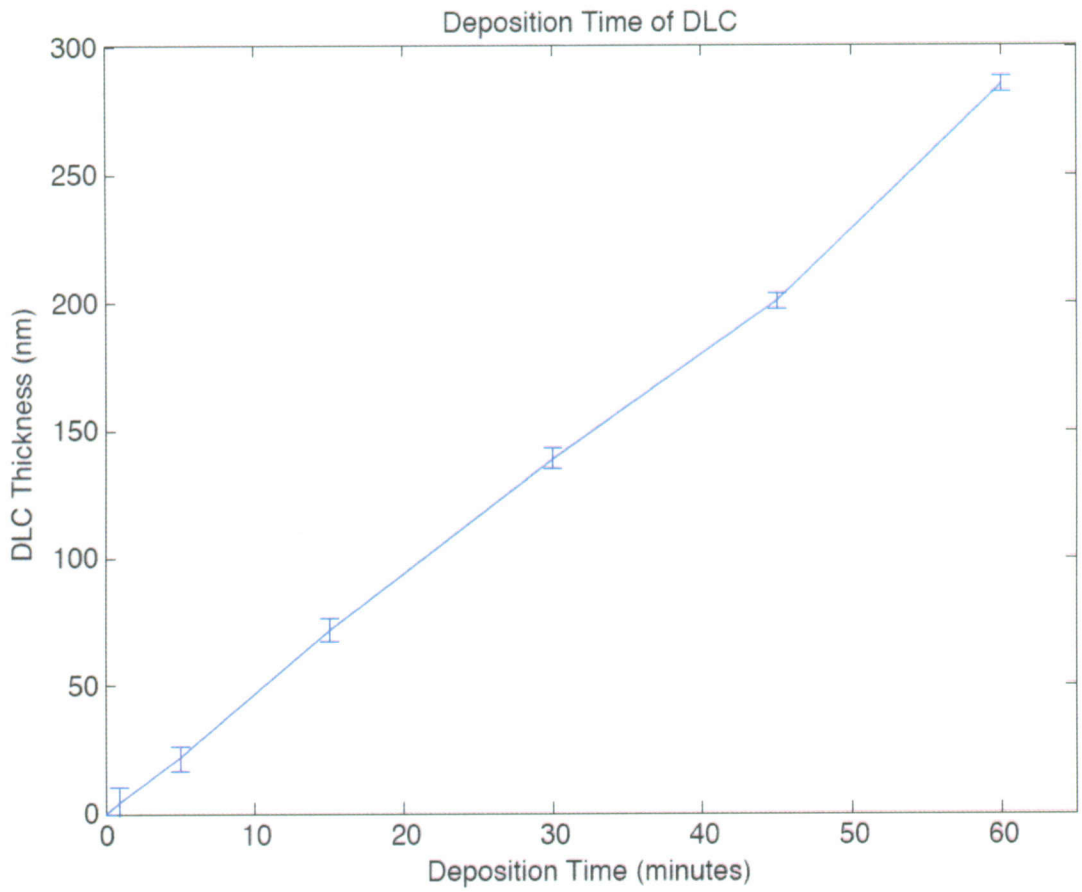


**Figure 3-1 - DLC thickness as a function of deposition time; Forward Power: 200W, Bias Power: 30W, Pressure: 6mTorr, Flow Rates: 3:1 Ar:$H_2$.**

Deposition times are for the entire rotating tray where samples are only exposed to the deposition at a fraction of the deposition time. The thicknesses of the DLC films were measured using an Ambios XP-2 profilometer post sputter deposition on multiple samples to determine the accuracy of the deposition technique with the rotating tray. Figure 3-1 clearly shows there is no significant delay time in which the film needs to nucleate on the surface.

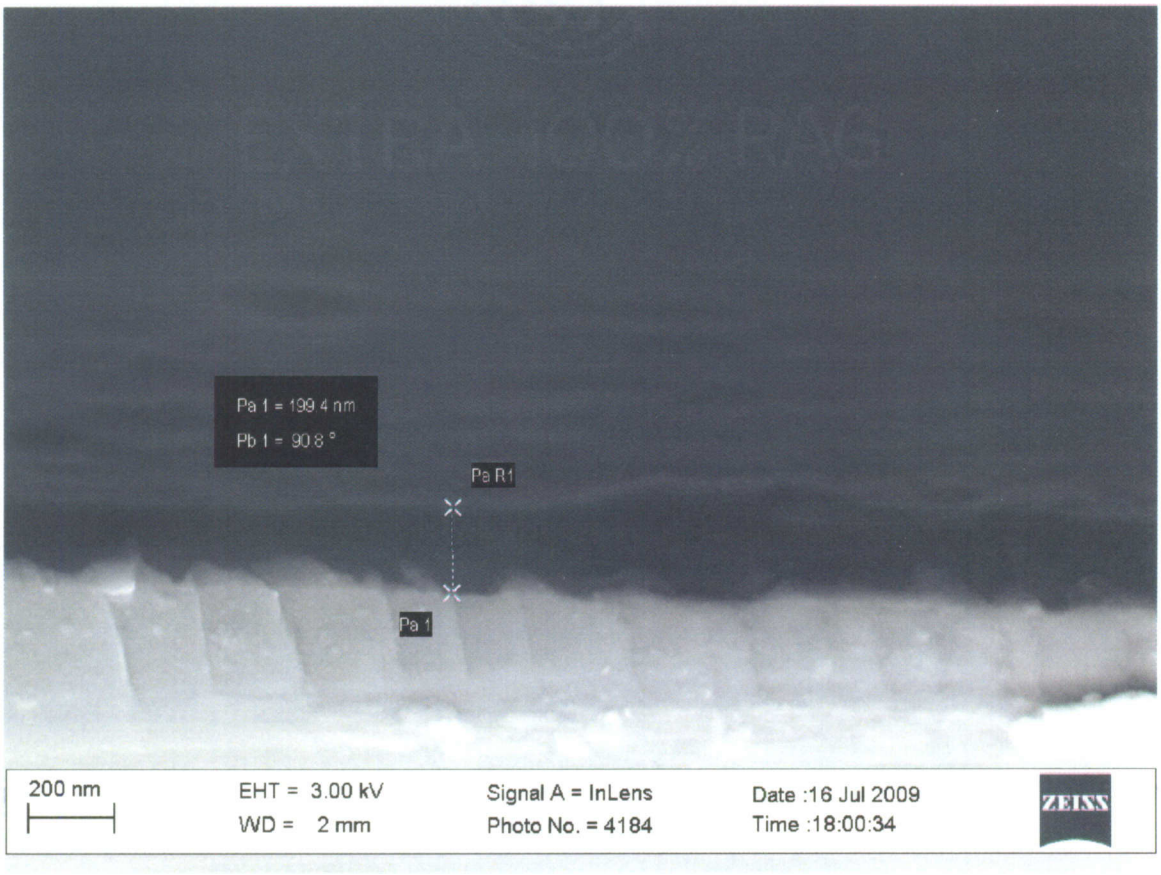


**Figure 3-2 - 200nm thick DLC on $SiO_2$/Si.**

Figure 3-2 clearly shows the smooth DLC layer on top of the $SiO_2$/Si. This also shows that the DLC film was uniform across the substrate. The ripples seen in Figure 3-2 may be present due to the high pressure DLC deposition technique. High pressure was used to ensure that the DLC would sputter onto the substrate at higher angles. No signs of this ripple effect were seen in the ultra-thin DLC layers.

## 3.6 Properties of Ultra-Thin DLC

The DLC films on $SiO_2$ were analyzed with an Atomic Force Microscope (AFM) and a Scanning Electron Microscope (SEM) to determine surface roughness and degree of pattern resolution decrease. When the ultra-thin DLC is sputter deposited onto the imprinter, the DLC layer will build up on the surface and sidewalls of the features on the imprinter. This increases the resolution of the features on the imprinter proportional to the thickness of the DLC deposited. It was determined that the surface was very smooth with less than 1nm RMS in roughness using an AFM and verified visually using the SEM. Since the surface energy of the surface of the imprinter is very important for an anti-adhesion layer, the Sessile Drop technique was used to determine the contact angle of the surface [15]. The contact angle characterizes the interfacial tension between a solid and a liquid drop. A hydrophilic surface would have a very low contact angle because the surface energy of the solid is greater than the liquids surface energy. A hydrophobic surface, on the other hand, would form a higher contact angle since the surface of the solid has a low surface energy that is much less than the surface tension of the liquid. The Sessile Drop technique is a method of contact angle measurements that utilizes optics to measure the angle of a drop on the substrate that is level. The surface contact angle with de-ionized (DI) water at room temperature of the DLC in this research was confirmed to be 60° as seen in prior DLC research. This means that the DLC surface still has a high surface energy and poor anti-adhesion capabilities for NIL. It should be noted that the contact angle would, in general, be a function of the material that is in the liquid. For example, alcohols, oils, and $H_2O$ will have different contact angles. Measuring the contact angle with $H_2O$ does not directly correspond to the imprinting

material, i.e. PMMA well above the glass transition temperature. However, a high contact angle for $H_2O$ on DLC and F-DLC surfaces has been shown, in previous work, to directly correspond to a low surface energy on the substrate [10].

The "Tape Test" (ASTM D3359) was utilized to measure the adhesion strength of each of the thin films to the $SiO_2$/Si substrate. This technique uses an adhesive tape that is applied to the film and pulled off to determine the adhesion strength. The test was performed on the thin DLC layer applied to the $SiO_2$/Si substrate. Our tests indicate that DLC on $SiO_2$ (thermally oxidized Si) show no evidence of peeling, liftoff, or cracking under the adhesion tape test.

## 3.7 Summary

The deposition technique in this research has not been thoroughly investigated. However, the most desirable properties in the DLC layer is the carbon to carbon bonding in the ultra-thin DLC layer. It has been proved in previous DLC research that the sputter deposition technique provides a possible method to keep the hardness and strength properties of DLC even with ultra-thin layers. Although these properties are not crucial to this work towards a universal NIL imprinter coating, if the DLC is able to provide more strength to the imprinter it can help protect the features on the imprinter from ripping and sticking to the sample or breaking. The surface energy of the DLC is lower than the surface energy of $SiO_2$, but it is still not quite low enough to provide a durable anti-stick layer for NIL. The next chapter provides the analysis of a second coating of fluorine to help lower the surface energy of the DLC layer even more with the use of $CF_4$ plasma in a RIE.

# CHAPTER 4

## Fluorinated Diamond-Like Carbon on Silicon Dioxide

### 4.1 Chapter Overview

This chapter discusses the many advantages and disadvantages of a Fluorinated Diamond-Like Carbon (F-DLC) layer. Previous work is reviewed on the hydrophobic nature of F-DLC films and the correlation between fluorination and the degree of being hydrophobic is analyzed. A method is also introduced for treating the surface of the ultra-thin DLC film mentioned in the previous chapter to lower the surface energy while retaining the mechanical stability of the fluorinated surface.

### 4.2 Introduction

Fluorine is the most electronegative element in the periodic table and when bound to carbon, it forms one of the strongest bonds in organic chemistry. This high electro-negativity leads to a high polarization of fluorine and applies a high electrostatic characteristic to the C-F bond. Fluorine is highly polarized $F^{\partial-}$ and carbon is highly polarized $C^{\partial+}$ resulting in a stable C-F bond that suppresses lone pair donation from fluorine [16]. This is a desirable characteristic in an anti-adhesion layer and proves to lower the surface energy of DLC significantly. This characteristic is applied to the ultra-thin DLC layer through the deposition of a monolayer of fluorine on top of the amorphous carbon. The processing of this deposition technique is discussed utilizing a Reactive Ion Etcher (RIE) and $CF_4$ plasma that is known to have an etching or deposition

rate depending on the environment variables. The fluorine is also known as a dopant for DLC and is minimized through environment variables in the RIE. The doping of the DLC with fluorine could affect the strength of the ultra-thin DLC layer. While this is not desired, it also does not affect the anti-stick characteristics of the fluorine layer. Figure 4-1 shows DLC in a basic amorphous state. Figure 4-2 shows this same amorphous DLC after being doped, deposited, and etched with fluorine.

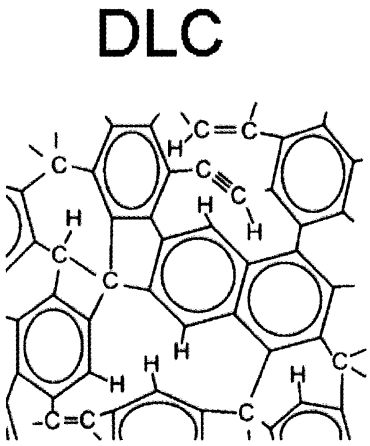


**Figure 4-1 - Diamond-Like Carbon structure.**

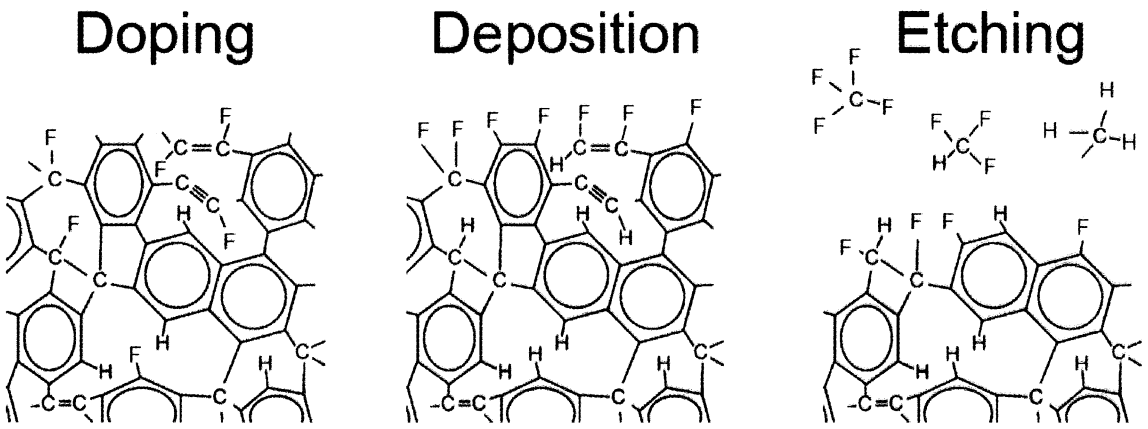


**Figure 4-2 - Chemical representation of doping, deposition, and etching DLC.**

## 4.3 C-F Bonding

The C-F bond is a highly polarized bond that gives the C-F bond an electrostatic characteristic. This creates a large dipole that interacts with other dipoles that are in the vicinity. However, this polarized bond does not give the C-F bond good donor ability. The three lone pairs of the fluorine that are bonded tightly to the carbon atoms cause a high electro-negativity of the configuration. For this reason, they typically will not interact as hydrogen bonding acceptors causing the C-F bond to be more hydrophobic in nature. The C-F bond is the strongest in organic chemistry at 105.4 kcal $mol^{-1}$.

## 4.4 Previous Work

The control of the hydrophobic nature of DLC surfaces has been studied through the use of $CF_4$ plasma etching and deposition along with the deposition of F-DLC [9]. The contact angle of DI water in air on DLC was shown to be around 60° in the previous chapter. The addition of fluorine as a dopant has also been shown to increase the hydrophobic nature of the surface to around that of PTFE and has been confirmed through a number of different works [9; 10; 17]. The contact angle of hydrocarbon-fluorocarbon mixtures depends on the chemical structure present where $-CF_2$ and $-CF_3$ groups showing a higher hydrophobic behavior than –CF as seen through different production techniques of F-DLC [9]. This chemical composition has been shown to depend heavily on the deposition conditions and plasma chemistry used in the RIE. Figure 4-3 shows the post DLC deposition CF4 treatment DI water contact angle when the RIE chamber pressure is varied. Increasing the pressure increases the contact angle of

the surface due to the increase in the level of hydrogenation (addition of hydrogen) of the DLC surface allowing for a higher degree of fluorination to occur (replacing C-H bonds with C-F bonds).

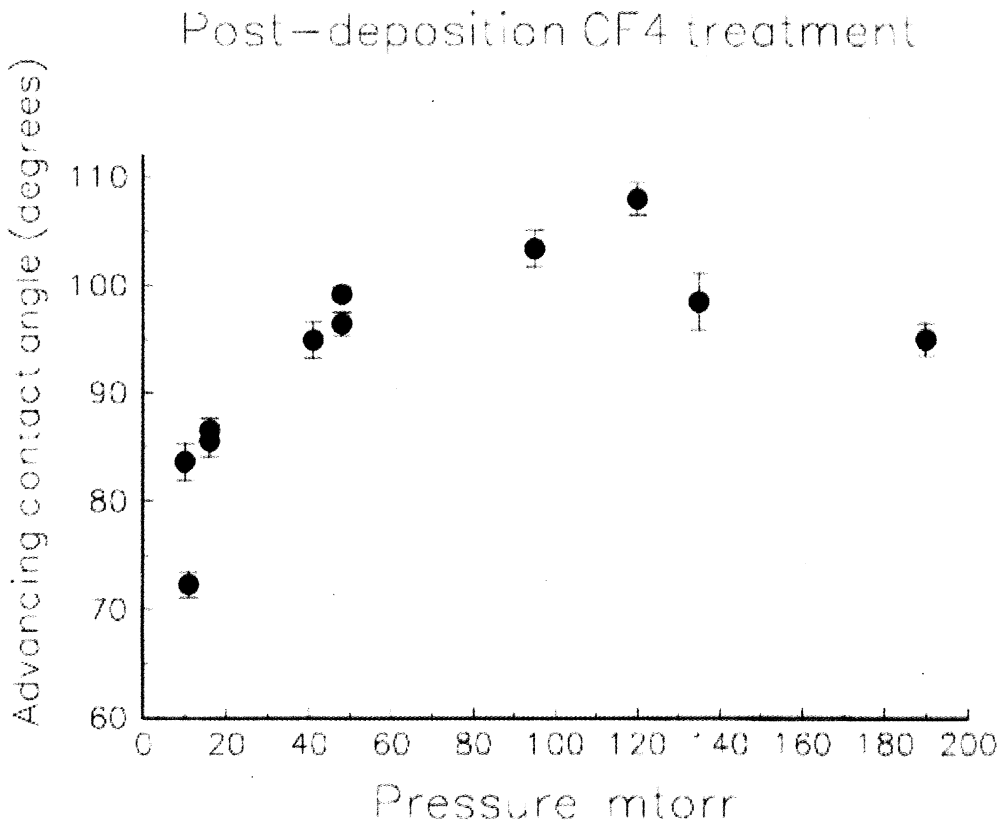


**Figure 4-3 - Contact angle of DI water on DLC treated with $CF_4$ at varying pressures [9].**

There has also been evidence that fluorine prefers to bond to $sp^3$ bonded carbon rather than $sp^2$ bonded carbon. Post fluorination technique, it has been shown that 75% of $sp^3$ bonds are fluorinated easily while only 30% of $sp^2$ bonds are fluorinated. Similar results to [9] in contact angle would prove that we have a large number of $sp^3$ bonds in our ultra-thin DLC layer.

## 4.5 Fluorination Technique

The DLC layer was fluorinated using a Plasmalab 80+ Reactive Ion Etcher (RIE) with $CF_4$ as the fluorine source. The $CF_4$ plasma has a known etch rate or deposition rate on the DLC layer [9] causing part of the DLC layer to become fluorinated or a monolayer of fluorine to be deposited onto the surface of the DLC. This etch rate or minimal deposition rate is desired in the imprinter fabrication to minimize the resolution decrease in the pattern on the imprinter. For $SiO_2$/Si imprinters, DLC is directly deposited onto the $SiO_2$. The fluorination of the DLC surface is then performed to lower the surface energy in the $CF_4$ plasma in the RIE. Due to the linearity and small etching rate of the DLC layer in the RIE $CF_4$ deposition technique, there is minimal (< 1nm) decrease in the resolution of the pattern on the imprinter. This decrease in resolution has been confirmed through the use of SEM imaging of actual imprinters that will be discussed in the next chapter.

## 4.6 Properties of Fluorinated DLC

The contact angle of these material layers was the primary focus of the layer testing using the Sessile Drop Technique as discussed previously. Results of the advancing contact angles with DI water are shown in this section. Figure 4-4 shows the advancing contact angle measurements for the $SiO_2$ substrate with both the DLC (lower line in figure) and F-DLC layers. The contact angle increases from an average of 65 degrees to 110 degrees with the application of the fluorinated layer and is independent of the DLC layer thickness.

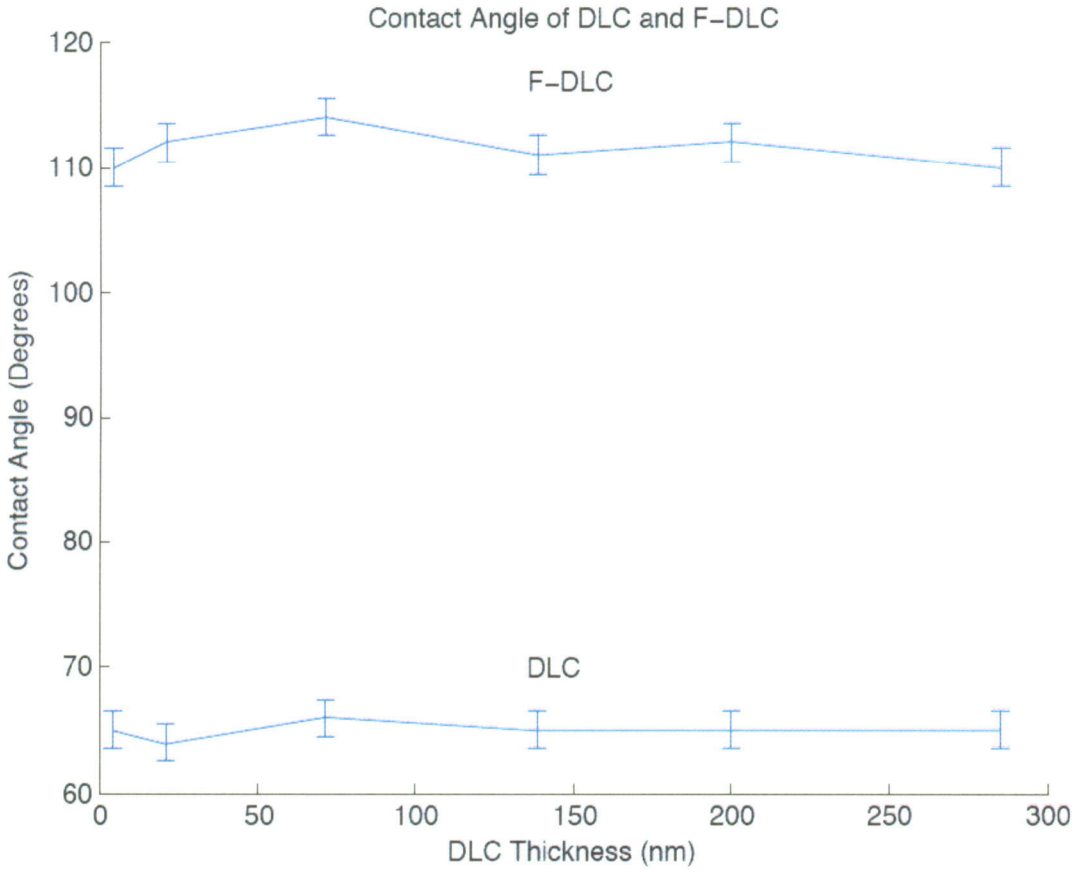


**Figure 4-4 - Contact angle in degress of DI water as a function of DLC thickness.**

The thinnest layer of DLC deposited was 3nm with an ultra-thin layer of fluorine above the DLC with minimal doping of the DLC surface. The contact angle measurements of a surface are known to depend on the surface morphology along with the chemical structure of the surface. For this reason, the surface contact angle measurements were performed on a plain silicon dioxide surface with a thin layer of DLC. This removes the possibility of pattern design or defects in the surface to provide an incorrect contact angle for the surface. Small features on the surface can alter the contact angle that is seen on a macro scale due to the increase in the surface area with the small features. In addition, the

surface morphology was not altered during the $CF_4$ fluorine treatment of the DLC layer and results are similar to previous work [9]. Figure 4-5 shows the DI water contact angle after each deposition step including the original $SiO_2$ on Si substrate. As can be seen, each step increases the contact angle and therefore lowers the surface energy of the imprinter pattern.

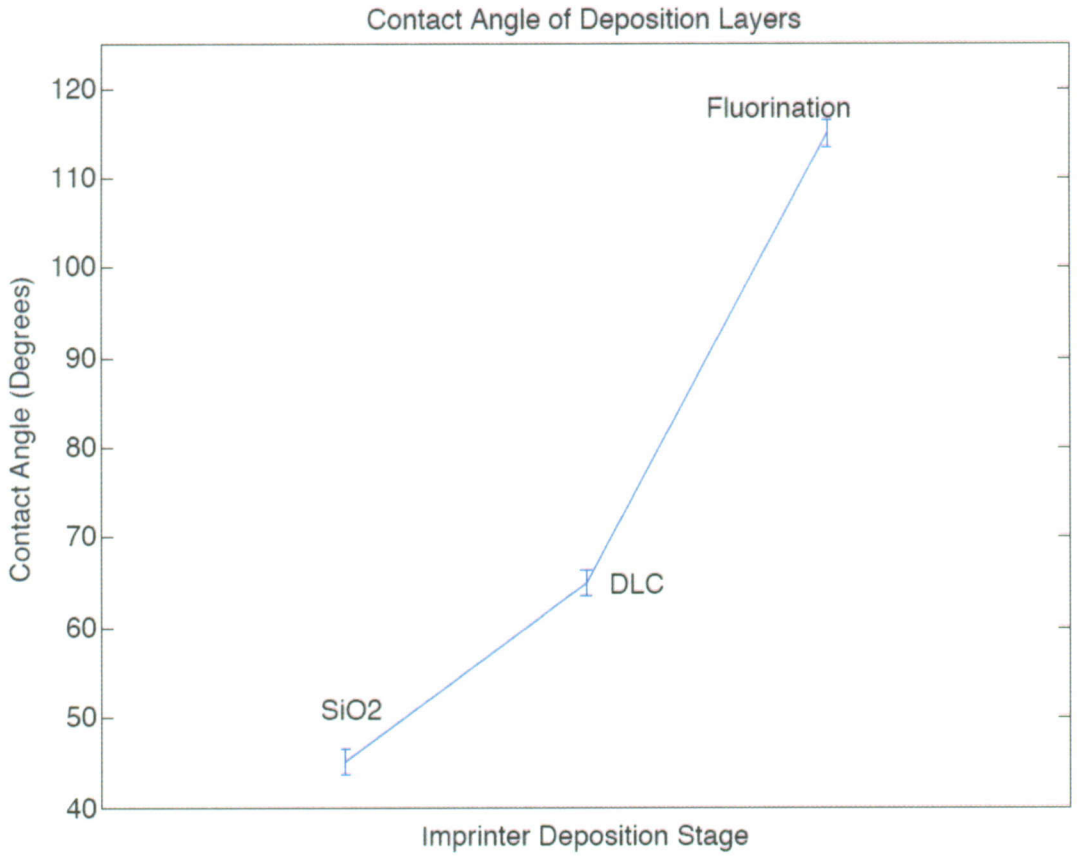


**Figure 4-5 – Contact angle of DI water after each deposition stage on a $SiO_2$/Si imprinter.**

An example of the contact angle measurement can be seen in the Figure 4-7 for a fluorine treated ultra-thin DLC layer on $SiO_2$/Si.

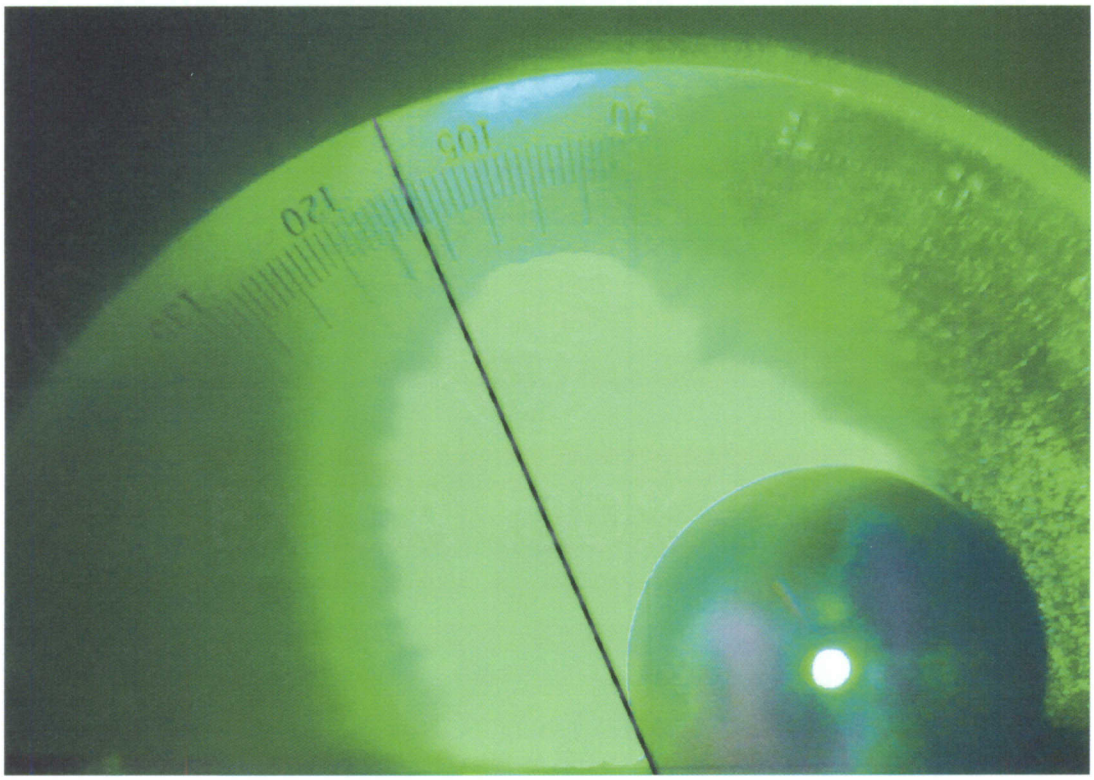

**Figure 4-6 – Sample measurement of contact angle of DI water on fluorine $CF_4$ treated DLC surface.**

The DI water contact angle on the $CF_4$ treated DLC proved to have extremely high angles between 112° and 115°. This shows that the surface energy of the ultra-thin F-DLC layer is less than 20mJ/m$^2$ and the ultra-thin DLC layer was a about 40mJ/m$^2$ as also seen in previous research [10]. The surface energy is calculated using the solid-liquid interfacial tension ($\gamma_{SL}$), the solid-vapour interfacial tension ($\gamma_{SV}$), and the liquid-vapour interfacial tension ($\gamma_{LV}$). These are all related to the contact angle through the Young equation $-\gamma_{SV} + \gamma_{SL} + \gamma_{LV}\cos\theta = 0$ [15]. The Good & Van Oss method models the surface energy of a solid ($\gamma_S$) as $\gamma_S = \gamma_S^d + 2\sqrt{\gamma_S^+\gamma_S^-}$ where $\gamma_S^d$ is the dispersive component (Lifshitz-Van der Waals interactions) and $\gamma_S^+, \gamma_S^-$ are the polar components. These components can then be related to each other with liquids ($\gamma_L$) that have known dispersive and polar

components as $\gamma_L(1+\cos\theta) = 2\left(\sqrt{\gamma_S^d\gamma_L^d} + \sqrt{\gamma_S^+\gamma_L^-} + \sqrt{\gamma_L^+\gamma_S^-}\right)$ [15]. To determine each of the components of the F-DLC surface, the contact angle was measured with DI water, glycerol, and ethylene glycol.

Di Water $$72.8\frac{mJ}{m^2}(1+\cos(112)) = 2\left(\sqrt{(\gamma_S^d)21.8\frac{mJ}{m^2}} + \sqrt{(\gamma_S^+)25.5\frac{mJ}{m^2}} + \sqrt{25.5\frac{mJ}{m^2}(\gamma_S^-)}\right)$$

Glycerol $$64.0\frac{mJ}{m^2}(1+\cos(98)) = 2\left(\sqrt{(\gamma_S^d)34\frac{mJ}{m^2}} + \sqrt{(\gamma_S^+)57.4\frac{mJ}{m^2}} + \sqrt{3.92\frac{mJ}{m^2}(\gamma_S^-)}\right)$$

Ethylene Glycol $$48.0\frac{mJ}{m^2}(1+\cos(87)) = 2\left(\sqrt{(\gamma_S^d)29\frac{mJ}{m^2}} + \sqrt{(\gamma_S^+)47\frac{mJ}{m^2}} + \sqrt{1.92\frac{mJ}{m^2}(\gamma_S^-)}\right)$$

Young Equation $$\gamma_S = \gamma_S^d + 2\sqrt{\gamma_S^+\gamma_S^-} = 17.3898 + 2\sqrt{0.120084 * 0.0934899} = 17.6017\frac{mJ}{m^2}$$

**Figure 4-7 - Sample surface energy calculation for the ultra-thin F-DLC layer.**

Through these four equations and four unknowns, the surface energy of the F-DLC can be determined. The surface energy for the F-DLC in this research was determined to be 17.6 mJ/m$^2$.

## 4.7 Summary

The C-F bond is one of the strongest bonds in organic chemistry and fluorine itself is the most electro negative element in the periodic table. This electro-negativity characteristic of fluorine gives the C-F bonds high electrostatic properties making it one of the best elements for anti-adhesion applications. The fluorine doping of DLC can weaken the

DLC layer through hydrogenation, replacing C-H bonds with C-F bonds. The chamber conditions with $CF_4$ plasma are extremely important. Not only can it change the deposition rate to an etching rate, but the chamber pressure also has a significant effect on lowering the surface energy of the DLC, or increasing the contact angle with DI water. In this chapter, a method for treating the surface of the ultra-thin DLC film was presented through the use of $CF_4$ plasma with specific chamber conditions. This layer was then analyzed with contact angle measurements to calculate the low surface energy of 17.6 $mJ/m^2$ similar to previous research with fluorinated DLC surfaces [10].

# CHAPTER 5

## Fluorinated Diamond-Like Carbon on $SiO_2$ Nanoimprinters

### 5.1 Chapter Overview

This chapter utilizes both the DLC and fluorination technique discussed in the previous two chapters to present a method for generating a $SiO_2$/Si nanoimprinter with the anti-adhesion layer applied. This technique is compared to previous work with entire DLC substrates performed at Columbia University [10]. It will also provide some insight into the durability and anti-stick properties of the new $SiO_2$/Si imprinters.

### 5.2 Introduction

DLC has been shown to have excellent adhesion to $SiO_2$ allowing for an ultra-thin DLC layer to be deposited on a $SiO_2$/Si imprinter. The fluorination of this DLC film in $CF_4$ plasma has also been shown to adhere and at the same time lower the surface free energy of the DLC film. This is very desirable in a nanoimprinter to ensure the imprinted polymer does not stick to the imprinter upon withdrawal of the imprinter. $SiO_2$ imprinters are the most widely used form of imprinter due to its use of silicon and the ease of fabrication. Other anti-stick layers have been used with these imprinters in the past [5], but their reliability is partial at best while being difficult to apply. The use of a DLC layer and a fluorination technique provides a simple method for application of the anti-adhesion layer with increased reliability. Another advantage of the F-DLC layer coating is that the reapplication of this coating is possible on $SiO_2$ imprinters.

## 5.3 Previous Work

Previous F-DLC anti-adhesion layers have been applied to DLC substrate imprinters [10]. One advantage of this technique is that the DLC substrate can provide a much harder imprinter and may be able to support the imprinting patterns. This work has shown that the advantages of DLC for imprinting include its mechanical strength, low surface energy, and its ability to be etched in an oxygen-based plasma. They also proved that DLC substrates have a surface energy around 40 $mJ/m^2$ and the fluorinated DLC surfaces have a surface energy around 20 $mJ/m^2$ when the DLC films were 100-200nm thick on Si substrates or were the entire substrate. The contact angle with DI water relating to the surface energy measurements for the DLC and F-DLC was around 100° due to the use of $C_4F_6$ and $C_4F_8$ plasmas. A disadvantage of using an entire DLC substrate is the cost and availability of high quality DLC substrates.

## 5.4 Imprinter Creation Technique

The creation of a $SiO_2$ imprinter was covered previously in this thesis, but a brief overview of the imprinter steps can be seen in Figures 5-1, 5-2, and 5-3. From left to right and top to bottom, the imprinter substrate is first coated with two separate layers of PMMA, 100k and 950k in 2% chlorobenzene. The SEM is then used to expose the e-beam sensitive resist with the electron beam controlled by a NPGS system as seen in stage 1.

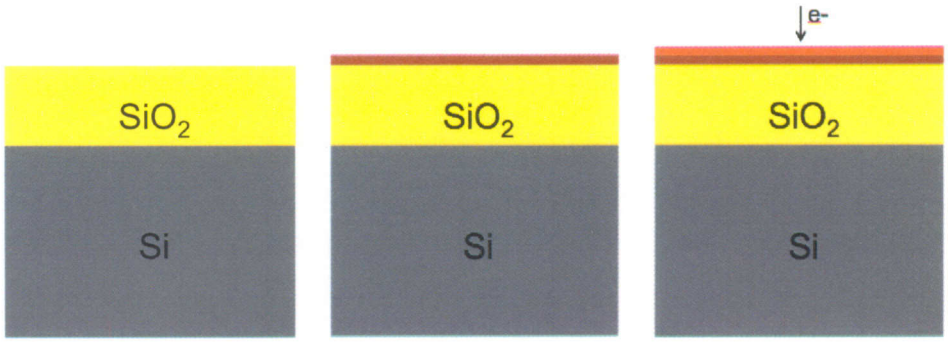


**Figure 5-1 - $SiO_2$ processing, stage 1.**

The exposed e-beam resist (PMMA) is then developed removing the exposed resist and leaving the $SiO_2$ exposed in the pattern desired. This step is then followed by the deposition of a thin (~20nm) layer of chrome while ensuring that there is no connection between the Cr on the $SiO_2$ and the Cr on top of the PMMA. The PMMA is then lifted off leaving the Cr layer on top of the $SiO_2$ in the desired pattern as seen in stage 2.


**Figure 5-2 - $SiO_2$ processing, stage 2.**

The substrate is then anisotropically etched in a $CF_4$ and $H_2$ plasma in a RIE about 100nm with the chrome protecting the $SiO_2$ below it in the pattern desired. The final processing for the $SiO_2$ imprinter is to remove the chrome surface with ceric ammonium nitrate leaving the desired pattern in the $SiO_2$ as seen in stage 3.

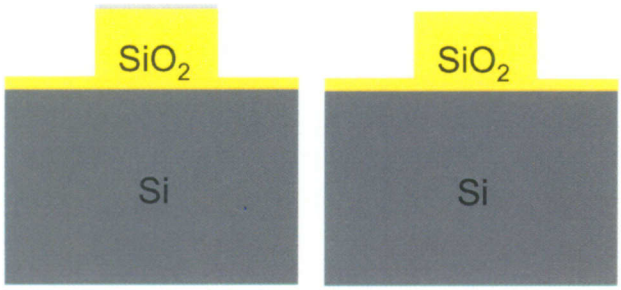


**Figure 5-3 – $SiO_2$ processing, stage 3.**

Once the $SiO_2$ imprinter pattern is created in the $SiO_2$ surface, the anti-adhesion F-DLC layer can then be applied. Figure 5-4 shows a graphical representation of the processing of the DLC and fluorination techniques. From left to right, the imprinter is etched using typical $SiO_2$ imprinter fabrication. Then the ultra-thin (< 5 nm) DLC film is applied to the surface and side walls of the $SiO_2$ imprinter using the sputter deposition system as discussed before. Finally, this $SiO_2$ imprinter with DLC coating is then placed in the RIE for the deposition of fluorine.

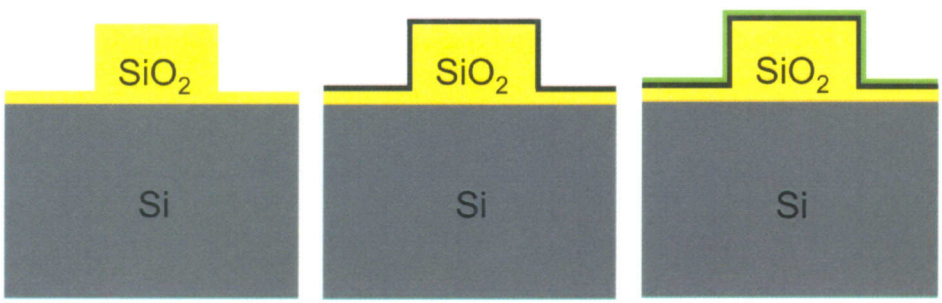


**Figure 5-4 - $SiO_2$ imprinter anti-adhesion F-DLC application.**

As can be seen in Figure 5-4, the DLC and fluorine layers coat all sides of the $SiO_2$. This is a result of the nature of sputtering for the DLC and the proper chamber conditions with

the RIE. It is very important to coat the sidewalls along with the surface since the majority of the adhesion between the imprinted polymer and the imprinter occurs on the sidewalls.

## 5.5 Ultra-Thin DLC and Fluorinated Layers

The ultra-thin DLC and fluorinated layers have been applied to imprinters with various features sizes. While it is difficult to recognize the difference between DLC and fluorine treated DLC, the application can be seen by a slight color change in the DLC surface of a gold/copper hue to a greenish blue hue as seen in Figure 5-5.

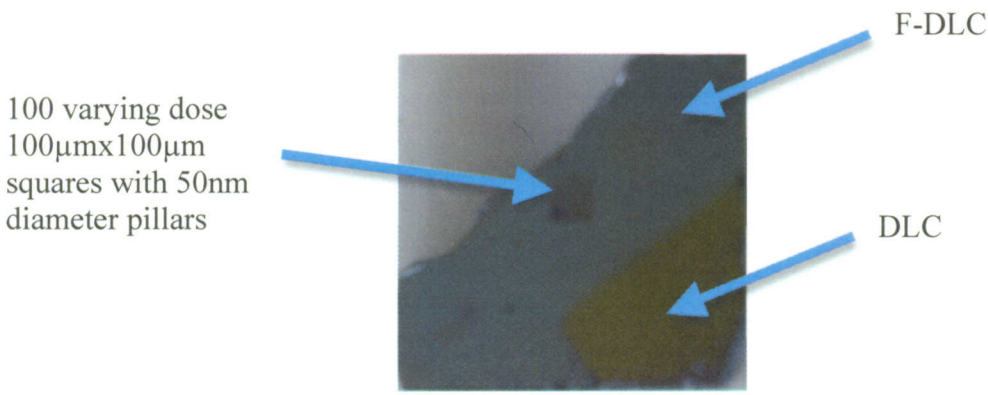


**Figure 5-5 – Optical micrograph of $SiO_2$ imprinter with DLC (Gold) and F-DLC (blue-green) areas.**

This color difference is due to the difference in thickness of the DLC and F-DLC film or the change in the refractive index for the F-DLC layer. These optical properties of thin films are generated through the interference and reflection of light waves as then reflect and pass through the DLC and F-DLC layers. The color also changes with the view angle of the observer to generate an effect that is known as iridescence. Figure 5-6 shows a 50 nm feature size imprinter with a thin (< 5 nm) coating of DLC. The sides of the pillar

walls show up in the SEM as a brighter color while the top and bottom of the imprinters have a darker hue to them.

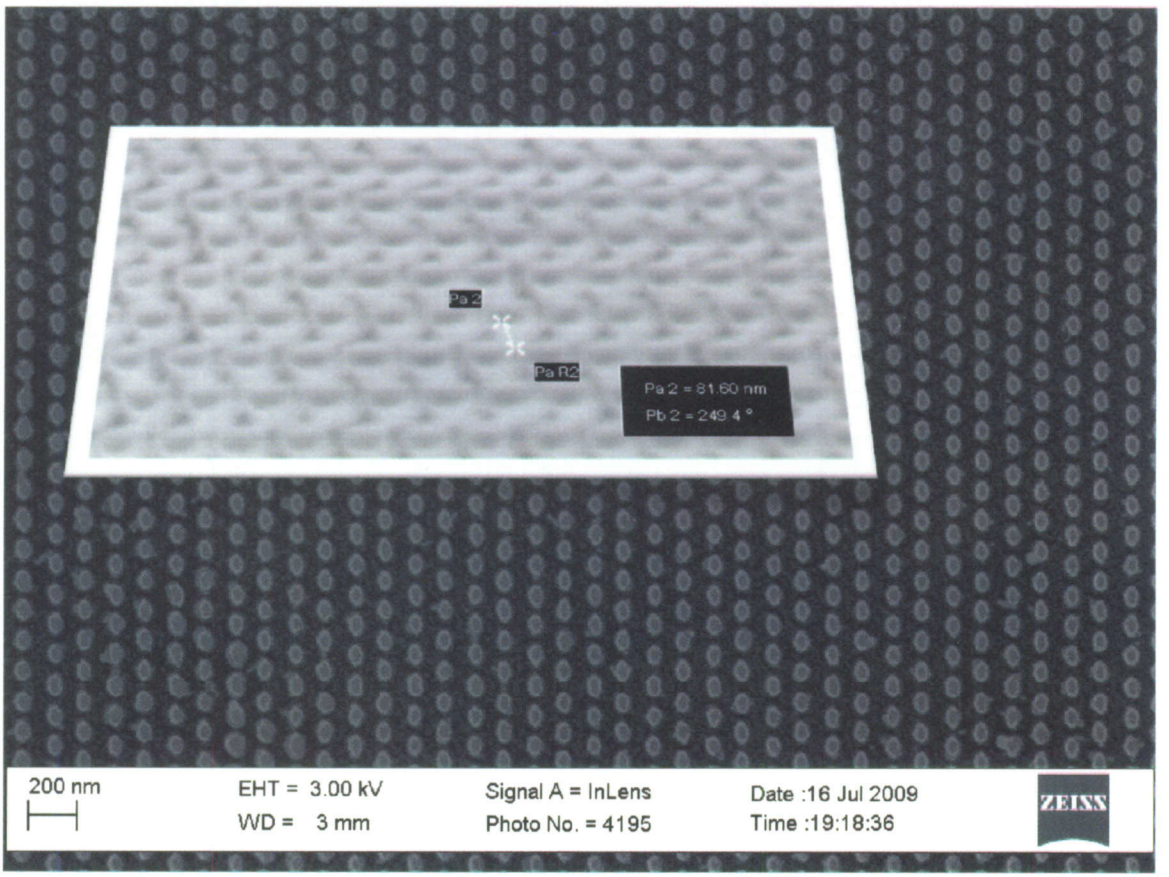


**Figure 5-6 – Top view and 45° angle view (inset) of an imprinter with an ultra-thin layer of DLC.**

Figure 5-7 shows the same imprinter with the ultra-thin DLC layer with an additional fluorine layer on top of the DLC with minimal thickness increase or resolution decrease.

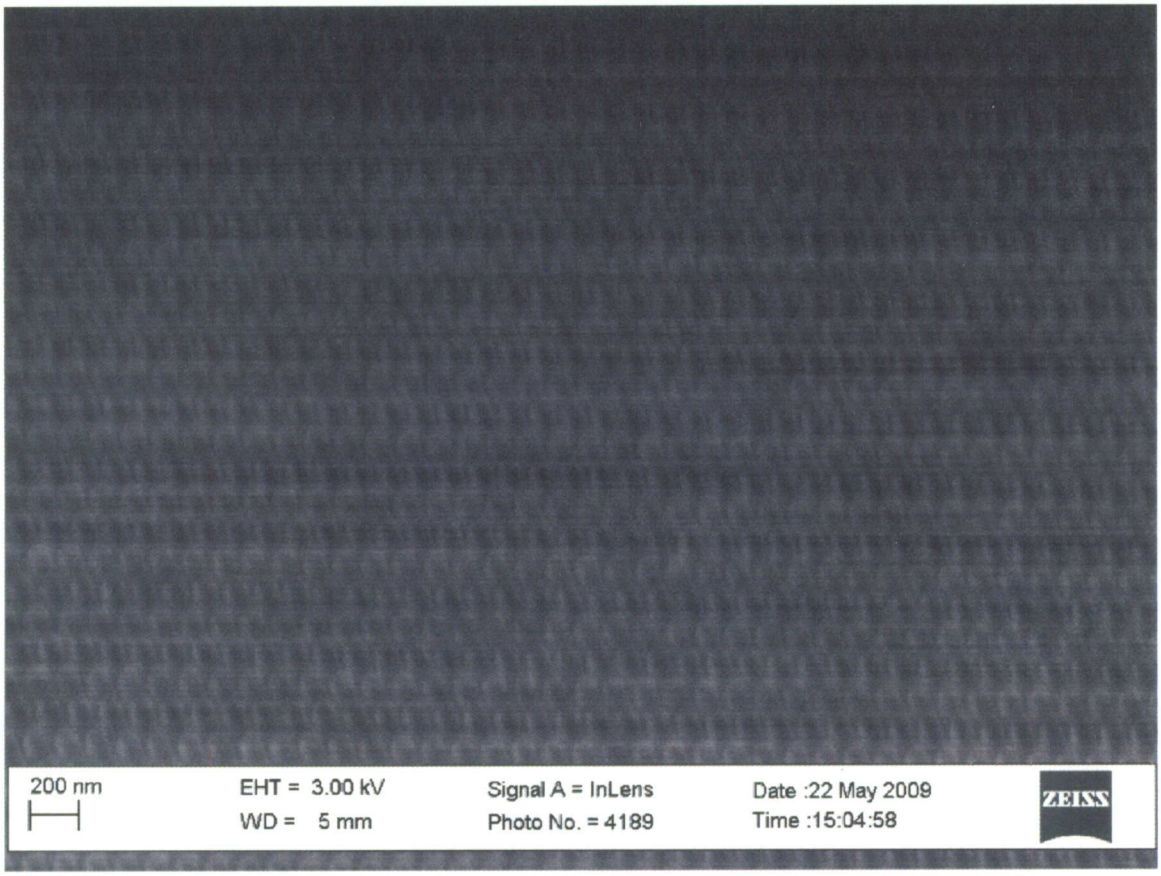


**Figure 5-7 – 45° SEM image of a $SiO_2$ imprinter with 50nm features with both DLC and fluorine ultra thin layers.**

## 5.6 Nanoimprint Lithography Resolution Loss

Typical resolution loss due to the anti-adhesion F-DLC layer is less than 5nm. This is due to the application of the DLC to the sidewalls of the pillars along with the top of pillars. If a larger feature size increase does not matter for the imprinter pattern, it may be beneficial to increase the thickness of the DLC layer on the imprinter. This has the potential to increase the strength of the DLC layer as mentioned in previous chapters. This thicker DLC layer has the added benefit of protecting the features while allowing for the re-application of the fluorination step multiple times without having to re-apply the DLC layer. Alternatively, the precision with which DLC can be deposited allows for

creating smaller gaps between features. While this has not been exploited in this work and is not the goal of this work, there are applications that could benefit from this technique.

The reapplication of the F-DLC layer on top of the DLC layer may amplify any defects in the DLC layer. To resolve this issue, the sample can be heated to 300˚C or placed in $O_2$ plasma. These two solutions have the ability to remove the DLC layer for re-application.

## 5.7 Imprinter Pattern Durability with F-DLC Coating

The F-DLC coating has proven to be a reliable and simple method for applying an anti-adhesion layer on $SiO_2$ imprinters. Multiple imprints with the same sample have been possible and the reapplication of the DLC and fluorinated surface is also possible. The visible color difference between the $SiO_2$, DLC, and F-DLC layers creates an easy method for determining the presence of the anti-adhesion layers.

The imprinter anti-adhesion F-DLC layer has been tested through multiple runs with comparisons to $SiO_2$/Si imprinting without an anti-adhesion layer. $SiO_2$/Si imprinters can produce good results but always result in portions of the PMMA sticking to the imprinter or the features on the imprinter tearing and being left in the sample PMMA. When the PMMA is not pre-baked to the sample, the adhesion of the PMMA to the imprinter is guaranteed. The pre-bake step helps create a good adhesion between the $SiO_2$ sample and the PMMA. Without the pre-bake, the PMMA attempts to adhere to both the imprinter and the sample equally resulting in adhesion to the imprinter. This proved to be a good test for the anti-adhesion layer since the PMMA was guaranteed to

stick to the imprinter. After multiple imprint attempts with the $SiO_2$/Si imprinter with the anti-adhesion layer, the pattern always transferred to the substrate without adhering to the imprinter even without the pre-bake step. Figure 5-8 shows an imprinted sample from a $SiO_2$ imprinter with the anti-adhesion F-DLC layer. As stated before, removing the pre-bake step from the sample processing may help with the flow of the PMMA and typically produces better results.

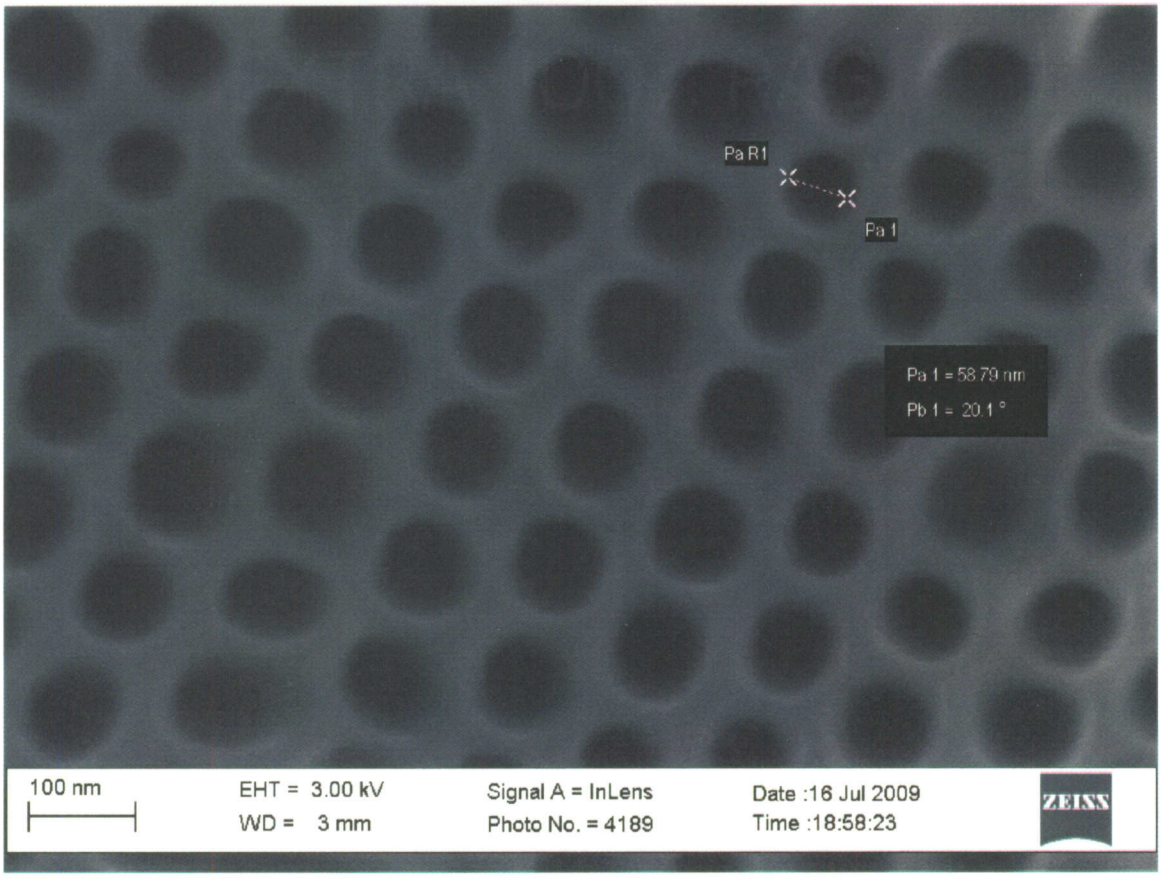


**Figure 5-8 - Imprinted PMMA by F-DLC $SiO_2$/Si imprinter.**

Figure 5-9 shows an image of the imprinter after ten imprints. All ten imprints resulted in good pattern transfer and minimal feature damage. After the tenth sample, the F-DLC layer was still intact on the surface of the imprinter and was determined visually through

the color of the imprinter.

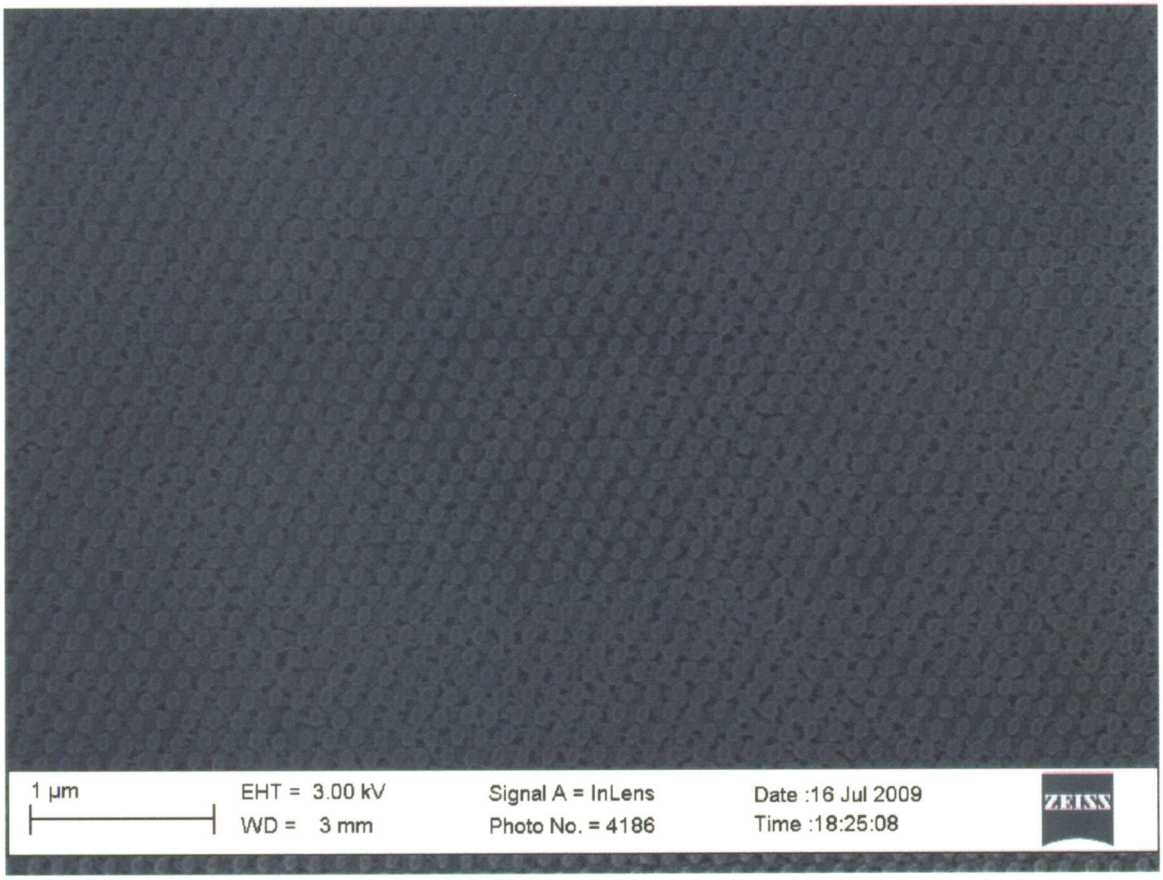


**Figure 5-9 - F-DLC $SiO_2$/Si Imprinter after 10 imprints.**

Quantitative analysis of imprinter reliability is difficult due to the large number of nanoscale features that need to be analyzed. Each imprinter created in this research contains 100 100µm x 100µm squares. Each of these squares contains about 1 million nanoscale features to be analyzed. Since there are 100 of these squares, there are 100 million nanoscale features that have to be analyzed over the surface of the imprinter. Since these features are on the scale of 30-50nm, the SEM must be used for analysis increasing the time needed to inspect each of the 100 million nanoscale features.

A secondary difficulty is that the optimal imprinting variables in the imprinting

process have not been finalized due to many variables in the current system design. To determine the optimal imprinting variables would require hundreds of imprints and the analysis of each imprint in the SEM. There is no definitive answer, at this time, to the question of how many imprints are possible before the imprinter needs to be replaced or re-coated.

Figure 5-10 shows multiple imprinting experiments, each with a new imprinter, and the result of the pattern transfer analyzed through optical lithography with the F-DLC coated imprinters. Results without the anti-adhesion F-DLC coating resulted in poor pattern transfer or imprinter destruction every time.

| | Temp | Pressure | Time | Prebake | Imprints | Results |
|---|---|---|---|---|---|---|
| Trial 1 | 160°C | 40 psi | 4 min | No | 10 | Pattern transfer was good for every imprint without adhering to the imprinter. The imprinter broke after 10 imprints due to uneven pressure. |
| Trial 2 | 170°C | 40 psi | 4 min | No | 12 | Pattern transfer was good for every imprint without adhering to the imprinter. Trial was ended after 12 imprints with a visible anti-adhesion layer still intact. |
| Trial 3 | 180°C | 40 psi | 4 min | No | 12 | Pattern transfer was good for every imprint without adhering to the imprinter. Trial was ended after 12 imprints with a visible anti-adhesion layer still intact. |
| Trial 4 | 180°C | 70 psi | 4 min | Yes | 0 | Imprinter temperature or pressure was not high enough for reliable pattern transfer. |
| Trial 5 | 190°C | 70 psi | 4 min | Yes | 0 | Imprinter temperature or pressure was not high enough for reliable pattern transfer. |
| Trial 6 | 200°C | 70 psi | 4 min | Yes | 0 | Imprinter temperature or pressure was not high enough for reliable pattern transfer. |
| Trial 5 | 210°C | 70 psi | 4 min | Yes | 5 | Imprinter broke after 5 imprints due to uneven pressure. |
| Trial 6 | 210°C | 80 psi | 4 min | Yes | 2 | Imprinter broke after two imprints due to uneven pressure. |

**Figure 5-10 - Trial runs for imprinters with and without the anti-adhesion F-DLC layers.**

## 5.8 Summary

This chapter has shown the application of the ultra-thin F-DLC anti-adhesion layer on a $SiO_2$/Si imprinter with a feature size increase of less than 5nm. The reapplication of the F-DLC and DLC layer has also been discussed through the removal of the DLC layer. After multiple imprint attempts, it may destroy parts of the F-DLC or DLC layers requiring the removal of both layers while protecting the $SiO_2$ imprinter features. The results presented in this chapter show excellent anti-adhesion properties through numerous tests and analysis through both an optical microscope and a SEM.

# CHAPTER 6

## Fluorinated Diamond-Like Carbon on Plastic

### 6.1 Chapter Overview

This chapter reviews the application of the ultra-thin F-DLC anti-adhesion layer on another imprinter material. Although this only shows one other type of imprinter material, the buffer layer technique described may be applicable to a large number of materials. While additional buffer layers slightly degrade the resolution of the imprinter, it offers the advantages of F-DLC to a wide range of imprinter materials and may lead to a universal anti-adhesion coating.

### 6.2 Introduction

The use of plastics as an imprinter material has a number of added benefits. Utilizing a rolling imprinting machine, the throughput of the pattern transfer of NIL can be drastically increased. These lithographic techniques require flexible material that can pass through a roller system while being strong enough to transfer the pattern into another material. This chapter discusses the application of the F-DLC anti-adhesion layer to a particular thermoplastic, polypropylene (PP), but the technique may be applicable to multiple types of flexible imprinters or imprinters that are very heat sensitive.

## 6.3 Roll-to-Roll Nanoimprint Lithography

Nanoimprint lithography has the potential to provide a cheap alternative to transfer nanometer-sized features on a large scale. However, current process and throughput of NIL is a limiting factor for many applications of the technique. Roller imprinting has been investigated in the past [18]. The main goal of this research was to allow the continuous printing of nanostructures on a flexible material with throughput that increases on the order of one or two magnitudes when compared to traditional NIL. The Roll-to-Roll Nanoimprint Lithography (R2RNIL) utilizes the same mechanical imprinting technique as NIL but utilizes flexible materials for the imprinter and the imprinted substrate. Besides the increased throughput of R2RNIL, it also requires less force to transfer a pattern while helping with the adhesion due to the rolling separation of the imprinter and the imprinted substrate.

R2RNIL does have a couple of important requirements. First, the imprinter mold needs to be generated on a flexible material. It needs to be flexible enough to wrap around a roller while having enough strength and durability to imprint other materials. On top of these requirements, the surface energy of the material must be low enough to promote anti-adhesion for continuous imprinting. In previous research, the fluoropolymer, ethylene-tetrafluoroethylene (ETFE) was used due to its high Young's modulus (1.2GPa) at room temperatures as a sample being imprinted by a rolling Si imprinter [18]. This imprinter system can be seen in Figure 6-1.

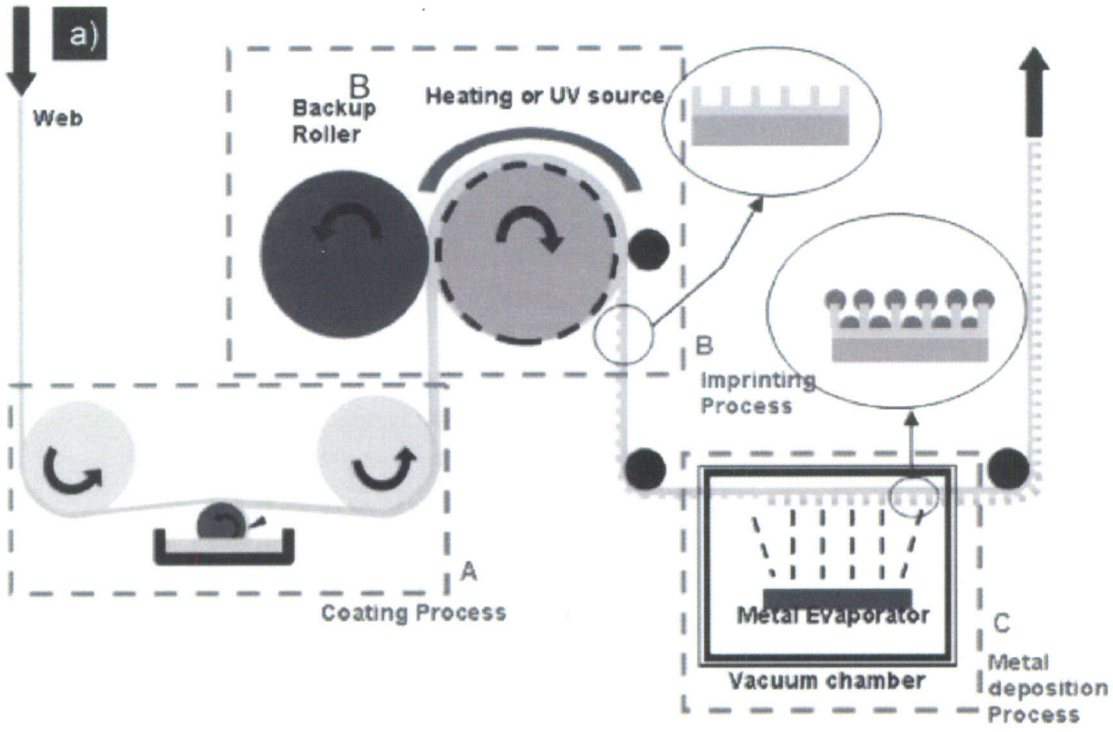


**Figure 6-1 - R2RNIL pattern transfer and evaporation design system [18].**

While this technique can increase the throughput of NIL, it limits the imprinting substrate to a flexible material. If this system were utilized in the reverse method, a flexible material for the imprinter and Si for the substrate, it could be applicable to the semiconducting industry. A flexible plastic based imprinter could be used along with a UV light source such as step-and-flash imprint lithography with Si wafers that roll on a conveyor system. While this system would provide a high throughput method of imprinting, it would require a method for providing strength to the plastic imprinter features while lowering the surface energy of the imprinter. For this portion of the research, the thermoplastic polypropylene (PP) is used although this deposition technique may be applicable to numerous other types of flexible thermoplastics.

## 6.4 Polypropylene

To test the anti-adhesion method on another imprinter material system, ultra-thin F-DLC was deposited onto PP using a glass buffer layer. The glass buffer layer is needed with thermoplastics to protect the features of the PP from the DLC sputter deposition stage. Figure 6-2 shows the PP deposition stages with the advancing contact angles of each stage. PP has a relatively high contact angle with DI water at 70 degrees and both the glass and DLC layers increase the surface energy of the PP and thus would increase the adhesion to the imprinted polymer. While this is an unwanted effect, the glass and DLC layers will help to protect and give strength to the PP features. The fluorination step then brings the contact angle of the surface back to 115 degrees indicating that the surface now has a low surface energy.

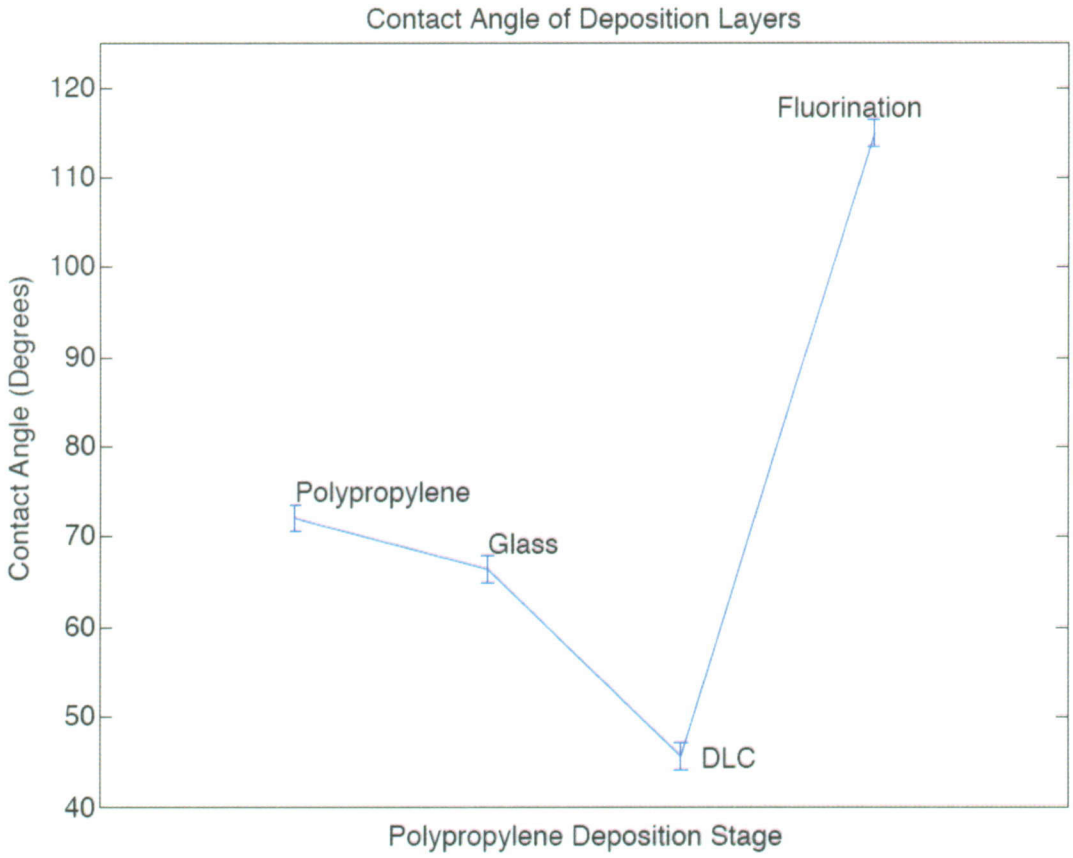


**Figure 6-2 - Contact angle in degress as a function of deposition stage for Polypropylene.**

## 6.5 Polypropylene Imprinter Fabrication

Polypropylene can be patterned using similar methods to $SiO_2$. Other methods of generating micro and nanostructured polypropylene surfaces include injection molding [19] and a novel form of imprinting that utilizes an imprinter of Si or $SiO_2$ on Si with a coating of PMMA that an adhesive PP then is attached to after cooling. When the adhesive PP is removed, the PMMA pattern separates from the imprinter leaving the pattern on the PP. This patterning process can be seen in Figure 6-3 [20].

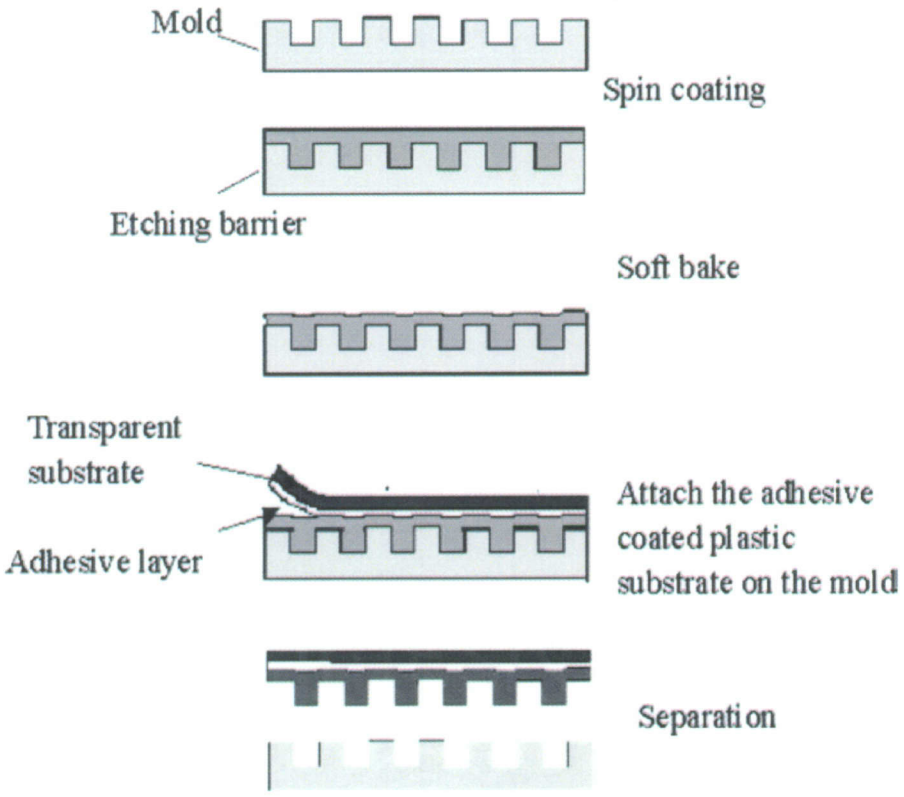


**Figure 6-3 - Polypropylene nanoimprint pattern transfer process for generating initial pattern [20].**

After the PP is patterned, the glass buffer layer is deposited followed by the DLC and fluorination techniques as seen in Figure 6-4 from left to right.

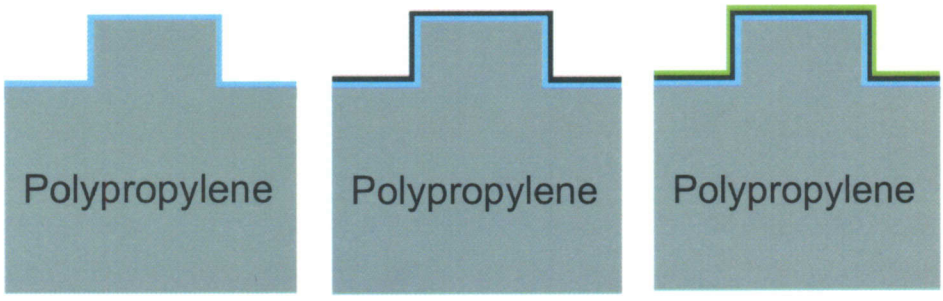


**Figure 6-4 - Polypropylene F-DLC anti-adhesion application. (Left: application of thin glass buffer layer, Center: Application of the DLC layer, Right: Fluorination of the DLC layer).**

Once the polypropylene is patterned, it can then be used as a UV R2RNIL. Since polypropylene has a melting temperature of about 160°C, it is not ideal for thermal NIL but this anti-adhesion layer is also applicable to other types of plastic or flexible materials that may allow for higher melting temperatures.

## 6.6 Summary

Flexible imprinters have the possibility to increase the throughput of NIL. R2RNIL has shown to be a technique for NIL that can utilize flexible materials for both the imprinter and the substrates. In this work, polypropylene was used to demonstrate the application of the ultra-thin F-DLC anti-adhesion layers to thermally sensitive plastics. These may benefit the area of R2RNIL with UV curing resist along with applications in a number of other areas where polypropylene is utilized. The glass buffer layer is used to protect the PP from the DLC deposition stage and allows for the fluorination of the DLC layer while protecting the PP. The glass buffer layer has excellent adhesion to the PP substrate and the DLC has excellent adhesion to the glass buffer layer.

# CHAPTER 7

# Conclusions

## 7.1 Chapter Overview

This chapter summarizes many of the conclusions that have been determined through this research work. Imprinter fabrication and implementation problems are addressed and the universal ultra-thin F-DLC layer is reviewed. Other imprinter coatings are also discussed and a few results from imprinting with and without the ultra-thin F-DLC layer are presented.

## 7.2 Imprinter Fabrication

DLC has been shown to be an excellent imprinter material when 100-200nm of DLC are used or the entire substrate is DLC. The fluorination of this DLC substrate was also discussed in previous research and shown to be an excellent method for lowering the surface energy of the imprinters. However, the use of strictly DLC based imprinters limits the fabrication methods for EBL and other techniques for generating nanometer scaled patters. This research focused on applying this same anti-stick technique to $SiO_2$ imprinters without weakening the structure of the $SiO_2$ features. $SiO_2$ imprinters were chosen because they are the most widely used imprinters. Feature sizes in NIL research go below 10nm and can be patterned over large areas in one step.

## 7.3 Imprinter Coatings

Current anti-adhesion layers were also addressed and have been utilized previously at Rowan University. It has been shown in the past that many of these techniques are unreliable and sometimes only provide marginal success. These techniques also require the modification of the chemistry of the surface of the $SiO_2$ while limited to $SiO_2$ imprinters due to the specific chemistry and most of these techniques are also very difficult to apply. They involve wet chemistry to modify end groups and usually require a dry box with water content << 1ppm. One major advantage of the F-DLC anti-adhesion layer presented in this work is that the re-application of the fluorine or even DLC layers is possible between imprinting steps.

## 7.4 Universal Imprinter Coatings

Many techniques have been used in nanoimprint lithography in an attempt to lower the surface free energy of the surface. The surface free energy is determined through the increase in the contact angle of the surface and determines the surface properties and the interfacial interactions including adsorption, wetting, and adhesion. It is desirable to have low adhesion of the surface of imprinters to ensure an accurate pattern transfer while retaining the pattern on the imprinter. An imprinter with high adhesion typically results in portions of the resist being torn from the imprinting sample as the imprinter is removed as seen in Figure 7-1. This destroys the sample and also may alter the pattern on the imprinter thus lowering the reproducibility of the pattern transfer.

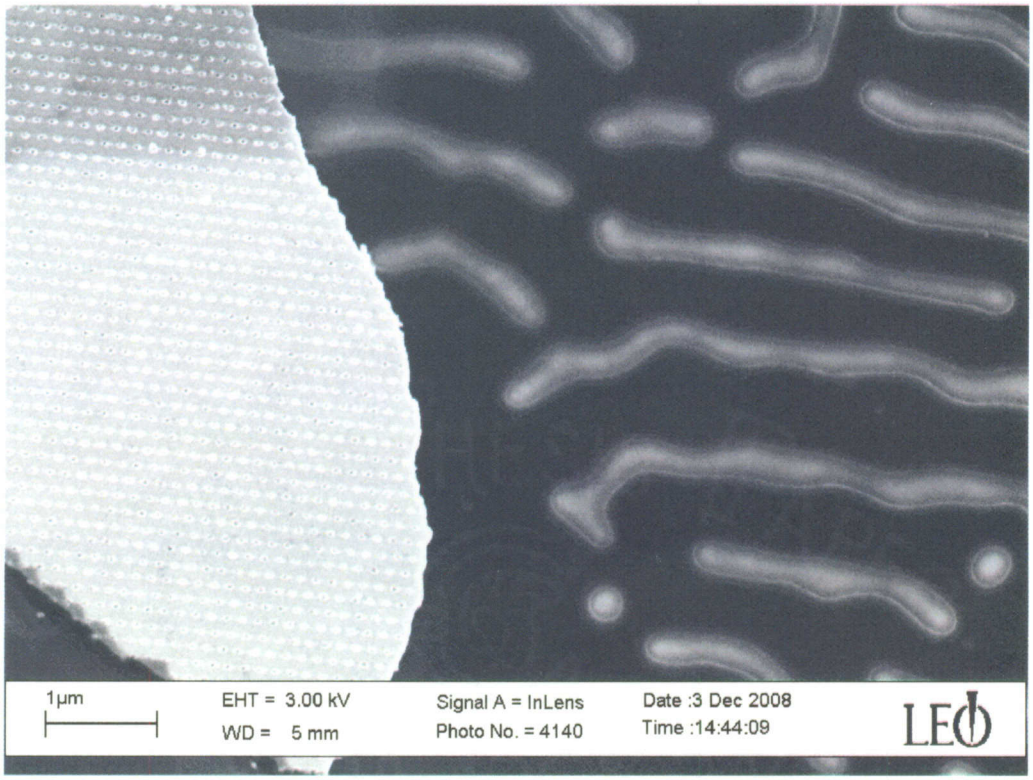


**Figure 7-1 - Imprinted sample without the F-DLC anti-stick coating on the imprinter. The left side of the image shows where the dot array transferred where the right side shows the missing PMMA that stuck to the imprinter.**

The F-DLC technique has been shown to be a reliable technique to minimize adhesion between the imprinter and the sample. The RIE processing also has minimal resolution decrease of the pattern on the imprinter. Using thick DLC substrates with a thin film of F-DLC as the imprinter has proven to retain the properties of DLC while allowing for a lower surface energy due to the thin F-DLC layer. However, requiring that the imprinter be DLC or F-DLC based greatly reduces the techniques allowed for the fabrication of the imprinter. Although this method utilizes an ultra-thin DLC layer, it still retains many of the important DLC properties needed for nanoimprint lithography. It also allows for the use of multiple imprinter generation techniques that could increase the possible resolution over DLC or F-DLC imprinters. However, the reapplication of both the DLC and the F-DLC layers may be required after multiple imprints for increasing the lifespan of the

imprinter.

## 7.5 Summary

Nanoimprint lithography is a viable technique for creating nanoscale features over large areas. Unfortunately, it is a contact technique and eliminating resist tearing and liftoff is critical for its success. Various imprinter material systems have been developed to achieve specific goals. However, these imprinters all have one thing in common – they must not adhere to the imprinted resist. Through the use of F-DLC, we have suggested a method for creating an anti-stick layer on a wide range of imprinter materials that has not been previously tested as an ultra-thin coating. On materials where DLC adheres well, fluorination significantly lowers the surface energy. On materials that do not promote DLC adhesion, we have demonstrated adhesion of DLC through the use of an ultra-thin $SiO_2$ buffer layer. This ultra-thin layer has been proven to retain a low surface energy approaching 17.6mJ/m$^2$ along with the strength of the DLC. Although the feature size of the initial imprinter is increased slightly due to the deposition of the anti-stick layers, the reliability of the imprinter increases allowing for a reliable transfer of smaller feature sizes.

## 7.6 Future Recommendations

A more in-depth analysis of the DLC layers may be important to address. Many of the deposition variables were not extensively varied in this work and it would be useful to determine if other deposition variables could increase the hardness or strength of the ultra-thin DLC layer.

The imprinting press design of the imprinter system at Rowan University could also have a couple modifications performed. First off, the water-cooling on the system could be re-connected to increase the pattern transfer speed of the NIL imprinter. One issue that should be addressed is the slightly non-uniform pressure of the two parallel plates. The $SiO_2$ wafers are not always perfectly flat with the two parallel plates and can cause the substrates to not apply uniform pressure like some of the commercially available imprinting systems. One reason for this is the use of the 9mm carbon tabs that are used for sticking the $SiO_2$/Si wafers to the top and bottom of the imprinter press. A solution that utilizes a vacuum to hold the samples in place could provide a more reliable imprint when uniform pressure is considered.

Although this ultra-thin F-DLC technique has excellent anti-adhesion properties, it has only been applied to two separate imprinter materials, $SiO_2$/Si and PP. Future research should attempt to apply the F-DLC coating to multiple imprinter types such as SiC, $Si_3N_4$, Ni, quartz, other plastics, and other flexible imprinter types.

## References


[1] D. J. Resnick, W. J. Dauksher, D. Mancini, K. J. Nordquist, T. C. Bailey, S. Johnson, N. Stacey, J.G. Ekerdt, C. G. Willson, S. V. Sreenivasan, and N. Schumaker. "Imprint Lithography: Lab Curiosity or the Real NGL?," SPIE, June 2003.

[2] R. Doering, Y. Nishi. *Handbook Of Semiconductor Manufacturing Technology*, Boca Raton : CRC Press, 2008.

[3] LaPedus, M. "Intel Drops 157-nm Tools from Lithography Roadmap," EETimes, May 2003.

[4] K. Suzuki, B. W. Smith. *Microlithography Science and Technology*, 2nd ed. Boca Raton : CRC Press, 2007.

[5] Marks, D. "The Implementation of Nanoimprint Lithography for the Fabrication of Patterned Magnetic Media," Rowan University, Glassboro, 2005.

[6] Corning Inc., "MACOR® Machinable Glass Ceramic," [Online] http://www.corning.com. [Accessed: June 29, 2009]

[7] C. Chu, G. N. Parsons. "Solvent Enhanced Resist Flow for Room Temperature Imprint Lithography," J. Vac. Sci. Technol. B, vol. 24, no. 2, pp. 818-822, March 2006.

[8] T. Bailey, B. Smith, B. J. Choi, M. Colburn, M. Meissl, S. V. Sreenivasan, J. G. Ekerdt, C. G. Willson. "Step and Flash Imprint Lithography: Defect Analysis," J. Vac. Sci. Technol. B, vol. 19, no. 6, pp. 2806-2810, Nov/Dec 2001.

[9] R.S. Butter, D.R. Waterman, A.H. Lettington, R.T. Ramos, E.J. Fordham. "Production and Wettings Properties of Fluorinated Diamond-Like Carbon Coatings," Thin Solid Films, vol. 311, no. 1-2, pp. 107-113, 1997.

[10] M. Schvartzman, A. Mathur, Y. Kang, C. Jahnes, J. Hone, and S. J. Wind. "Fluorinated Diamond-Like Carbon Templates for High Resolution Nanoimprint Lithography," J. Vac. Sci. Technol. B, vol. 26, pp. 2394-2398, 2008.

[11] Grove, R. "A Patterning Process Utilizing Nanoimprint Lithography for Fabrication of Planar Perpendicular Patterned Magnetic Media," Rowan University, Glassboro, 2005.

[12] P. Lemoine, J. P. Quinn, P. D. Maguire, J. F. Zhao, J. A. McLaughlin. "Intrinsic Mechanical Properties of Ultra-Thin Amorphous Carbon Layers," Applied Surface Science, vol. 253, no. 14, pp.6165-6175, 2007.

[13] S. Aisenberg, R. Chabot. "Ion Beam Deposition of Thin Films of Diamond Like Carbon," J. Appl. Phys., vol. 42, 1971.

[14] D. A. Outka, W. L. Hsu, K. Phillips, D. R. Boehme, N. y. C. Yang, D. K. Ottesen, H. A. Johnsen, T. J. Headley, W. M. Clift. "Compilation of Diamond-Like Carbon Properties for Barriers and Hard Coatings," Sandia National Laboratories, Albuquerque, 1994.

[15] R. Ranganathan "Surface Activity and Effects as Measured by Contact Angle," Texas Tech University, Lubbock, 2003.

[16] D. O'Hagan. "Understanding Organofluorine Chemistry. An Introduction to the C-F Bond," Chemical Society Reviews, vol. 37, pp. 308-319, 2008.

[17] M. Beck, M. Graczyk, I. Maximov, E.-L. Sarwe, T. G. I. Ling, M. Keil, and L. Montelius. "Improving Stamps for 10nm Level Wafer Scale Nanoimprint Lithography," Microelectron. Engr., vol. 61-62, pp. 441-448 (2002).

[18] S. H. Ahn, L. J. Guo. "High-Speed Roll-to-Roll Nanoimprint Lithography on Flexible Plastic Substrates," Advanced Materials, vol. 20, pp. 2044-2049, 2008.

[19] T. Rasilainen, M. Suvanto, T. A. Pakkanen. "Anisotropicaly microstructured and micro/nanostructured polypropylene surfaces," Surface Science, vol. 603, pp. 2240-2247, 2009.

[20] W. Liao, S. L. Hsu, S. Chu, P. Kau. "Imprint Lithography for Flexible Transparent Plastic Substrates," Microelectronic Enginering, vol. 75, pp. 145-148, 2004.

[21] A. Grill. "Diamond-Like Carbon: State of the Art," Diamond Relat. Mater., vol. 8, pp.428-434, 1999.

[22] M. Grischke, K. Bewilogua, K. Trojan, H. Dimigen. "Application Oriented Modifications of Deposition Processes for DLC-Based Coatings," Surf. Coat. Technol, vol. 2, no. 74/75, pp. 739-745,1995.

[23] R. Memming. "Properties of Polymeric Layers of Amorphous Hydrogenated Carbon Produced by a Plasma-Activated Chemical Vapour Deposition Process I: Spectroscopic Investigations," Thin Solid Films, vol. 143, no. 3, pp. 279-289 1986.

[24] S. Ramachandran, L. Tao, T. H. Lee, S. Sant, L. J. Overzet, M. J. Goeckner, M. J. Kim, G. S. Lee, and W. Hu. "Deposition and Patterning of Diamond-Like Carbon as Anti-Wear Nanoimprint Templates," J. Vac. Sci. Technol. B, vol. 24, pp. 2993-2997, 2006.

[25] J.-K. Chen, F.-H. Ko, K.-F. Hsieh, C.-T. Chou, and F.-C. Chang. "Effect of Fluoroalkyl Substituents on the Reactions of Alkylchlorosilanes with Mold Surfaces for Nanoimprint Lithography, J. Vac. Sci. Technol. B, vol. 22, pp. 3233-3241, 2004.